Versatile Routes to Mono- and Bis(alkynyl) Manganese(II) and Manganese(III) Complexes via Manganocenes

Dieter Unseld, Vassily V. Krivykh,† Katja Heinze, Ferdinand Wild, Georg Artus, Helmut Schmalle, and Heinz Berke*

Institute of Inorganic Chemistry, University of Zürich, Winterthurerstrasse 190, 8057 Zürich, Switzerland

Received December 29, 1998

With the manganocenes $(RC_5H_4)_2Mn$ (R = H, Me) as starting materials, paramagnetic d^5 half-sandwich complexes $(RC_5H_4)Mn(dmpe)(C{\equiv}CR')$ (dmpe = 1,2-bis(dimethylphosphino)-ethane; R = Me, R′ = Ph, **1a**; R = Me, R′ = $SiMe_3$, **2a**; R = H, R′ = Ph, **1b**; R = H, R′ = $SiMe_3$, **2b**) have been prepared by the reaction with terminal or $SnMe_3$-substituted acetylenes and dmpe. The derivatives **1a** and **2a** could be isolated, while **1b** and **2b** have been identified in mixtures with the bis(dmpe)bis(acetylide)manganese species **3** (R′ = Ph) and **4** (R′ = $SiMe_3$). The latter compounds are obtained as the sole products, when the manganocenes are reacted with dmpe and the corresponding acetylenes in a 1:2:2 ratio. **1a** and **2a** can be reversibly oxidized to the corresponding cationic Mn(III) complexes $[(MeC_5H_4)Mn(dmpe)(C{\equiv}CR')][BF_4]$ (R′ = Ph, $[\mathbf{1a}]^+$; R′ = $SiMe_3$, $[\mathbf{2b}]^+$). Compounds **1a** and **2a** act as scavengers of H• radicals in the 1:1:1 reaction mixtures or in the presence of *n*-Bu_3SnH or $(C_5Me_5)Mo(CO)_3H$, forming the vinylidene species $(MeC_5H_4)Mn(dmpe)(=C=C(H)R')$ (R′ = Ph, **5**; R′ = $SiMe_3$, **6**). In the absence of a special H• donor, **1a** slowly dimerizes to give the binuclear complex **7**. A similar process occurs with $[\mathbf{1a}]^+$ to form the bis(carbyne) complex **8**. **8** can be reduced to **7** by a reaction with 2 equiv of $(MeC_5H_4)_2Co$, and in turn **7** can be oxidized to **8** with 2 equiv of a ferrocenium salt. Equal amounts of **7** and **8** comproportionate to afford the mixed-valence complex $[\mathbf{7}]^+$. If applicable, the new compounds have been characterized by spectroscopic (NMR, EPR, near-IR) and electrochemical measurements, as well as X-ray diffraction studies (**2a**, **5**, **7**, and **8**) and DFT calculations.

Introduction

The first representatives of the manganocene family $(C_5H_5)_2Mn$ and $(MeC_5H_4)_2Mn$ have been known for around 40 years.[1] Their electronic properties, especially the high-spin/low-spin crossover, have attracted much attention and have been studied extensively by photoelectron[2] and EPR[3,4] spectroscopy, by magnetic measurements in solution,[3] by electron diffraction,[5] and by NMR spectroscopy.[3,6] The manganocenes have the longest M−C distances and exhibit the highest reactivity of all metallocenes of the 3d transition-metal series.[5] They are pyrophoric, hydrolyze instantaneously in contact with water and acids,[1b] undergo facile ring exchange reactions characteristic of ionic cyclopentadienide compounds,[7] and allow substitution of one cyclopentadienyl ligand by three two-electron donors, e.g. L = CO[8] or L = $P(OR)_3$.[9] The mechanism of the last reaction is presumably more complicated than a simple one-step replacement of a cyclopentadienyl group, as redox processes with L as a reducing agent are sometimes involved. The analogous reaction with L = PMe_3 does not proceed at all;[9] instead, the tertiary phosphine adducts $(R'C_5H_4)_2Mn(PR_3)$ (R′ = H, Me; R_3 = Me_3, Et_3, Me_2Ph, $MePh_2$) are formed.[10] The chelating bis(phosphine) $Me_2PCH_2CH_2PMe_2$ (1,2-bis(dimethylphosphino)-ethane, dmpe) even gives rise to adducts with coordination of both phosphorus atoms.[10] The 1:1 adducts with the more electronegative donors 3,5-dichloropyridine[11] and tetrahydrofuran[12] have "tilted" planar cyclopenta-

† Present address: Nesmeyanov Institute of Organoelement Compounds, Vavilov Street 28, V-334, Moscow, Russia 117813.

(1) (a) Fischer, E. O.; Leiphinger, H. *Z. Naturforsch.* **1955**, *B10*, 353. (b) Wilkinson, G.; Cotton, F. A.; Birmingham, J. M. *J. Inorg. Nucl. Chem.* **1956**, *2*, 95.

(2) (a) Rabalais, J. W.; Werme, L. O.; Bergman, K. L.; Karlsson, L.; Hussain, M.; Siegbann, K. *J. Chem. Phys.* **1972**, *57*, 1185. (b) Evans, S.; Green, M. L. H.; Jewitt, B.; King, G. H.; Orchard, A. F. *J. Chem. Soc., Faraday Trans.* **1974**, *2*, 356. (c) Cauletti, C.; Green, J. C.; Kelly, M. R.; Powell, P.; van Tilborg, J.; Robbins, J.; Smart, J. *J. Electron Spectrosc. Relat. Phenom.* **1980**, *19*, 327.

(3) Switzer, M. E.; Wang, R.; Rettig, M. F.; Maki, A. H. *J. Am. Chem. Soc.* **1974**, *96*, 7669.

(4) (a) Ammeter, J. H.; Bucher, R.; Oswald, N. *J. Am. Chem. Soc.* **1974**, *96*, 7833. (b) Ammeter, J. H. *J. Magn. Reson.* **1978**, *30*, 299.

(5) Almeningen, A.; Haaland, A.; Samdal, S. *J. Organomet. Chem.* **1978**, *149*, 219.

(6) (a) Hebendanz, N.; Köhler, F. H.; Müller, G.; Riede, J. *J. Am. Chem. Soc.* **1986**, *108*, 3281. (b) Cozak, D.; Gouven, F.; Demers, J. *Can. J. Chem.* **1987**, 6, 1912. (c) Köhler, F. H.; Schlesinger, B. *Inorg. Chem.* **1992**, *31*, 2853.

(7) Switzer, M. E.; Rettig, M. F. *J. Chem. Soc., Chem. Commun.* **1972**, 687.

(8) Fischer, E. O.; Jira, R. *Z. Naturforsch.* **1954**, *B9*, 618.

(9) Werner, H.; Juthani, B. *J. Organomet. Chem.* **1977**, *129*, C39.

(10) Howard, C. G.; Girolami, G. S.; Wilkinson, G.; Thornton-Pett, M.; Hursthouse, M. B. *J. Am. Chem. Soc.* **1984**, *106*, 2033.

(11) Weed, J. T.; Rettig, M. F.; Wing, R. M. *J. Am. Chem. Soc.* **1983**, *105*, 6510.

(12) Bottomley, F.; Keizer, P. N.; White, P. S. *J. Am. Chem. Soc.* **1988**, *110*, 173.

10.1021/om9810549 CCC: $18.00
Publication on Web 03/25/1999

Scheme 1. Synthesis of 1a, 1b, 2a, 2b, 3, 4, [1a]$^+$, and [2a]$^+$

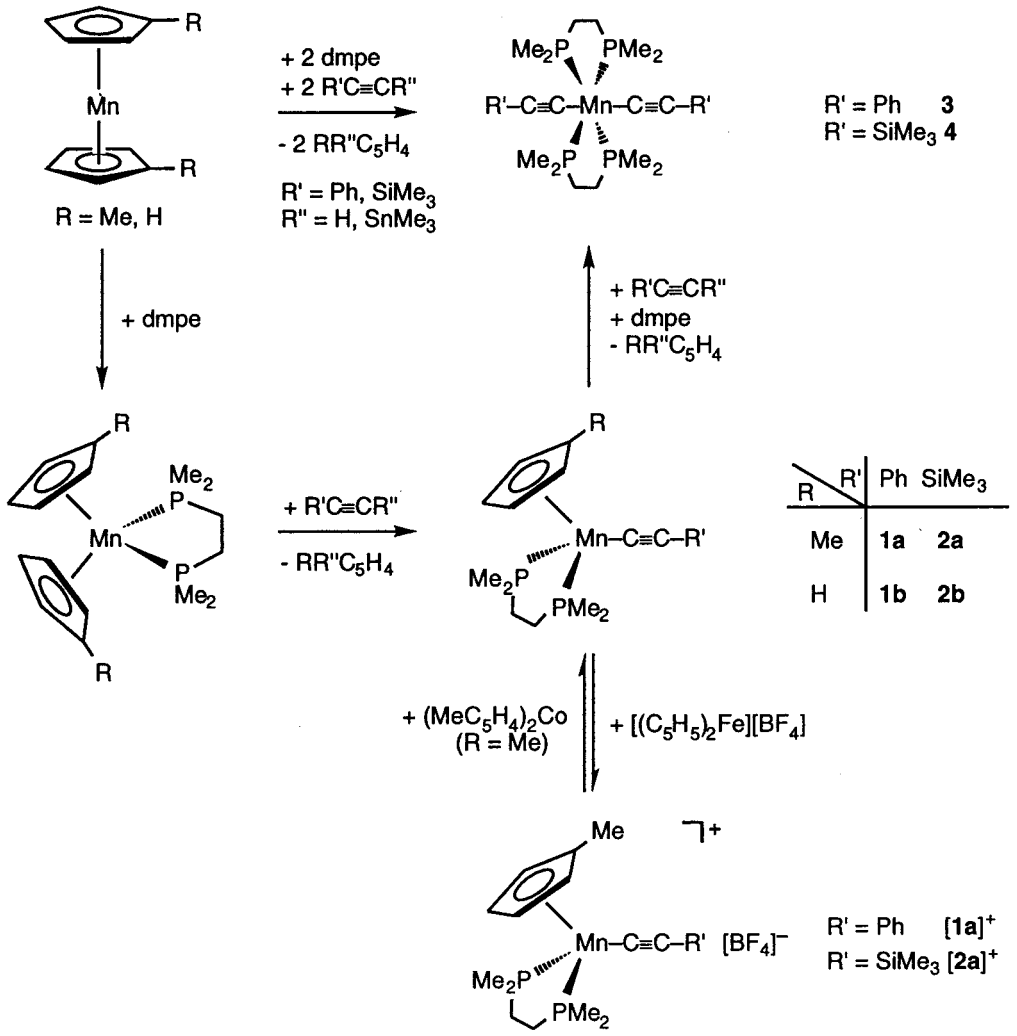

dienyl rings in the solid state. In contrast to the dmpe derivatives the tmeda (tetramethylethylendiamine) adduct contains an η^1-Cp ring.[13] Neither the electronic nature nor the chemical properties of these unusual, formally 19- and 21-valence-electron derivatives have been studied and exploited for chemical applications. Ligand exchange is also observed in the reaction of manganocene adducts with dihalides MnX_2, leading to binuclear halide-bridged $[(MeC_5H_4)MnL_2X]_2$ (L = PMe_3, PEt_3, $AsEt_3$; X = Cl, Br, I) or mononuclear complexes $(MeC_5H_4)MnL_2I$ (L_2 = $(PMe_3)_2$, dmpe).[14]

On the basis of the facile cyclopentadienyl replacement and the capability of adduct formation of manganocenes, we sought to develop a new manganocene chemistry by probing their reactions with terminal or trimethyltin-substituted acetylenes in the presence of dmpe.

Results and Discussion

Syntheses and Properties of Half-Sandwich Complexes $(RC_5H_4)Mn(dmpe)(C{\equiv}CR')$ (R = H, Me; R′ = Ph, $SiMe_3$; 1a,b and 2a,b). In the presence of dmpe manganocene and 1,1′-dimethylmanganocene react in a 1:1 ratio with terminal and trimethyltin-substituted alkynes R′C≡CR″ (R′ = Ph, $SiMe_3$; R″ = H, $SnMe_3$) with substitution of one five-membered ligand to form the alkynyl complexes **1a**,**b** and **2a**,**b** (Scheme 1).

Long reaction times are required for the formation of **1a** and **2a** from terminal alkynes (**1a**, 20 h; **2a**, 65 h), and even longer times are needed for the reaction starting from trimethyltin-substituted alkynes (**1a**, 30 h; **2a**, 80 h). In the latter transformations the cyclopentadienyl moieties are liberated as trimethyltin derivatives, as proven by NMR spectroscopy (see Experimental Section). The reverse reaction—formation of cyclopentadienyl transition-metal complexes via cleavage of a trialkyltin−cyclopentadienyl bond—is known for diamagnetic metal centers.[15]

The primary intermediates in these three-component transformations are the dmpe adducts $(RC_5H_4)_2Mn(dmpe)$, previously reported by Wilkinson et al.,[10] as shown by ^{1}H NMR spectroscopic studies in C_6D_6. As the dmpe ligand easily dissociates from this adduct (fast exchange on the ^{1}H NMR time scale), manganocenes are still present in the reaction mixture. The reaction

(13) Heck, J.; Massa, W.; Weinig, P. *Angew. Chem.* **1984**, *96*, 699; *Angew. Chem., Int. Ed. Engl.* **1984**, *23*, 722.
(14) Köhler, F. H.; Hebendanz, N.; Müller, G.; Thewalt, U. *Organometallics* **1987**, *6*, 115.
(15) (a) Abel, E. W.; Moorhouse, S. *J. Organomet. Chem.* **1971**, *29*, 227. (b) Abel, E. W.; Dunster, M. O.; Waters, A. *J. Organomet. Chem.* **1973**, *49*, 287. (c) Abel, E. W.; Moorhouse, S. *J. Chem. Soc., Dalton Trans.* **1973**, 1706.

sequence of Scheme 1 can be initiated from the adduct complexes and acetylenes, while no reaction is observed between manganocenes and acetylenes in the absence of dmpe, even under more forcing conditions. Therefore, the multistep reaction obviously proceeds via the dmpe adducts $(RC_5H_4)_2Mn(dmpe)$, giving the half-sandwich complexes **1a**,**b** and **2a**,**b**.

At this stage of the reaction sequence the R = H and R = Me derivatives behave differently. While the complexes **1a** and **2a** (R = Me) can be isolated in pure form, the more reactive species **1b** and **2b** (R = H) could only be detected in solution. Their enhanced reactivity, which parallels that of $(C_5H_5)_2Mn(dmpe)$ (the reaction of the latter with acetylenes proceeds faster than that of $(MeC_5H_4)_2Mn(dmpe)$, as shown by ^{1}H NMR monitoring in deuterated 1,2-dichloroethane), leads to further cyclopentadienyl substitution, giving **3** and **4**, respectively (Scheme 1). Obviously, the unsubstituted cyclopentadienyl ring is a better leaving group than the methylcyclopentadienyl ring in the $(RC_5H_4)_2Mn(dmpe)$ adducts as well as in the $(RC_5H_4)Mn(dmpe)(C{\equiv}CR')$ complexes.

For this reaction sequence starting from $(C_5H_5)_2Mn$ the bis(alkynyl) bis(dmpe) complexes **3** and **4** are seemingly the thermodynamic products. Presumably, the same is valid for the complexes with MeC_5H_4, and the isolation of **1a** and **2a** is only possible due to the kinetic inertness of these compounds.

Our previous investigations in this field have demonstrated that the bis(alkynyl)manganese complexes $Mn(dmpe)_2(C{\equiv}CR')_2$ (**3**, **4**) undergo reversible 1-electron-oxidation processes leading to 16-electron low-spin cations.[16] To explore the general accessibility of organometallic Mn(III) systems, we also examined the redox chemistry of the mono(alkynyl) derivatives **1a** and **2a**. The addition of 1 equiv of $[(C_5H_5)_2Fe](BF_4)$ to **1a** or **2a** resulted in the formation of the sensitive cationic species [**1a**](BF_4) and [**2a**](BF_4), respectively (Scheme 1). The complexes [**1a**](BF_4) and [**2a**](BF_4) were isolated in a pure state and characterized by spectroscopic, electrochemical, and magnetic means.

The IR spectra of **1a** and [**1a**](BF_4), recorded in KBr pellets, exhibit bands at 2008 and 2070 cm^{-1}, respectively, a region characteristic of the phenylethynyl $C_\alpha-C_\beta$ stretching mode.[17] The $\nu(C{\equiv}C)$ absorptions of the (trimethylsilyl)ethynyl derivatives are observed at much lower wavenumbers (1945 cm^{-1} for **2a**; 1995 cm^{-1} for [**2a**](BF_4)), which appears to be a typical feature of $SiMe_3$-substituted acetylide ligands and may suggest a weakening of their triple bond.[18] The wavenumber of the C≡C absorption increases upon oxidation of the metal center. The same observation was made for the bis(alkynyl) derivatives **3** and **4** in the Mn(II) and Mn(III) oxidation states[16] and also for compounds of the general type $[M(C{\equiv}CR)\{E(CH_2CH_2PPh_2)_3\}]^{n+}$ (M = Co, Rh; E = N, P), for which the ordering Co(III) > Co(II),[19] Rh(III) > Rh(II) > Rh(I)[20] was derived. These findings were interpreted in terms of enhanced π back-bonding to the acetylide unit in low-oxidation-state species. In certain cases oxidation of the metal center may have no[21] or even a reverse[22−24] effect on the stretching frequency of the attached acetylide ligand, which is inconsistent with the π back-bonding hypothesis, but a suitable interpretation is still lacking.

NMR spectra of paramagnetic complexes may provide useful information on their structures and electronic states.[25] To manganese complexes paramagnetic NMR has been applied in just a few instances, e.g. to the parent manganocenes and their substituted derivatives.[3,6] The chemical shifts of the methyl and methylene protons of the dmpe ligands are especially suited for assigning different spin states. For the high-spin complexes $(MeC_5H_4)Mn(dmpe)I$[14] and $Mn(dmpe)_2X_2$ (X = Br, I)[26] two broad downfield signals are observed for the methylene and the methyl groups of the dmpe ligand, while for the low-spin complexes $Mn(dmpe)_2X_2$ (X = Me,[26] C≡CR'[16]) these resonances are shifted to higher field strengths and the width at half-height of these signals is much smaller. For the low-spin Mn(III) cations $[Mn(dmpe)_2(C{\equiv}CR')_2]^+$ the upfield shift is even larger and the half-widths are about twice as large due to the presence of two unpaired electrons.[16]

In the ^{1}H NMR spectra of the $(RC_5H_4)_2Mn(dmpe)$ intermediates the chemical shifts of the signals of the dmpe and RC_5H_4 ligands were found close to those of the above-mentioned high-spin complexes, indicating a high-spin configuration for $(RC_5H_4)_2Mn(dmpe)$ in solution consistent with the observed crystallographic bond lengths and magnetic moments found in the solid state.[10]

Despite the large line widths, which cause in some cases overlap and integration problems, assignment of all resonances in the ^{1}H NMR spectra of **1a**, **2a**, $[\mathbf{1a}]^+$, and $[\mathbf{2a}]^+$ was possible. Due to the thermal instability of these complexes, the temperature could not be increased in order to induce sharpening of the signals. The complexes **1a** and **2a** have approximately the same

(16) Krivykh, V. V.; Eremenko, I. L.; Veghini, D.; Petrunenko, I. A.; Pountney, D. L.; Unseld, D.; Berke, H. *J. Organomet. Chem.* **1996**, *511*, 111.

(17) Manna, J.; John, K. D.; Hopkins, M. D. *Adv. Organomet. Chem.* **1995**, *38*, 79.

(18) Sun, Y.; Taylor, N. J.; Carty, A. J. *Organometallics* **1992**, *11*, 4293.

(19) (a) Bianchini, C.; Innocenti, P.; Meli, A.; Peruzzini, M.; Zanobini, F.; Zanello, P. *Organometallics* **1990**, *9*, 2514. (b) Bianchini, C.; Peruzzini, M.; Vacca, A.; Zanobini, F. *Organometallics* **1991**, *10*, 3697.

(20) (a) Bianchini, C.; Meli, A.; Peruzzini, M.; Vacca, A.; Laschi, F.; Zanello, P.; Ottaviani, F. M. *Organometallics* **1990**, *9*, 360. (b) Bianchini, C.; Laschi, F.; Ottaviani, F.; Peruzzini, M.; Zanello, P. *Organometallics* **1988**, *7*, 1660. (c) Bianchini, C.; Masi, D.; Meli, A.; Peruzzini, M.; Ramirez, J. A.; Vacca, A.; Zanobini, F. *Organometallics* **1989**, *8*, 2179. (d) Bianchini, C.; Mealli, C.; Peruzzini, M.; Vizza, F.; Zanobini, F. *J. Organomet. Chem.* **1988**, *346*, C53. (e) Bianchini, C.; Meli, A.; Peruzzini, M.; Zanobini, F. *J. Chem. Soc., Chem. Commun.* **1987**, 971. (f) Bianchini, C.; Meli, A.; Peruzzini, M.; Zanobini, F.; Zanello, P. *Organometallics* **1990**, *9*, 241.

(21) (a) Bianchini, C.; Laschi, F.; Masi, D.; Ottaviani, F. M.; Pastor, A.; Peruzzini, M.; Zanello, P.; Zanobini, F. *J. Am. Chem. Soc.* **1993**, *115*, 1175. (b) Bianchini, C.; Meli, A.; Peruzzini, M.; Frediani, P.; Bohanna, C.; Esteruelas, M. A.; Oro, L. A. *Organometallics* **1992**, *11*, 138.

(22) Connelly, N. G.; Gamasa, M. P.; Gimeno, J.; Lapinte, C.; Lastra, E.; Maher, J. P.; Le Narvor, N.; Rieger, A. L.; Rieger, P. H. *J. Chem. Soc., Dalton Trans.* **1993**, 2575, 2981 (correction).

(23) Bitcon, C.; Whiteley, M. W. *J. Organomet. Chem.* **1987**, *336*, 385.

(24) (a) Beddoes, R. L.; Bitcon, C.; Whiteley, M. W. *J. Organomet. Chem.* **1991**, *402*, 85. (b) Adams, J. S.; Bitcon, C.; Brown, J. R.; Collison, D.; Cunnigham, M.; Whiteley, M. W. *J. Chem. Soc., Dalton Trans.* **1987**, 3049.

(25) (a) *NMR of Paramagnetic Molecules*; La Mar, G. N., Horrocks, W. DeW., Holm, R. H., Eds.; Academic Press: New York, 1973. (b) Bertini, I.; Luchinat, C. *NMR of Paramagnetic Molecules in Biological Systems*; Benjamin-Cummings: Menlo Park, CA, 1986. (c) Bertini, I.; Luchinat, C. *Coord. Chem. Rev.* **1996**, 150.

(26) Girolami, G. S.; Wilkinson, G.; Galas, A. M. R.; Thornton-Pett, M.; Hursthouse, M. B. *J. Chem. Soc., Dalton Trans.* **1985**, 1339.

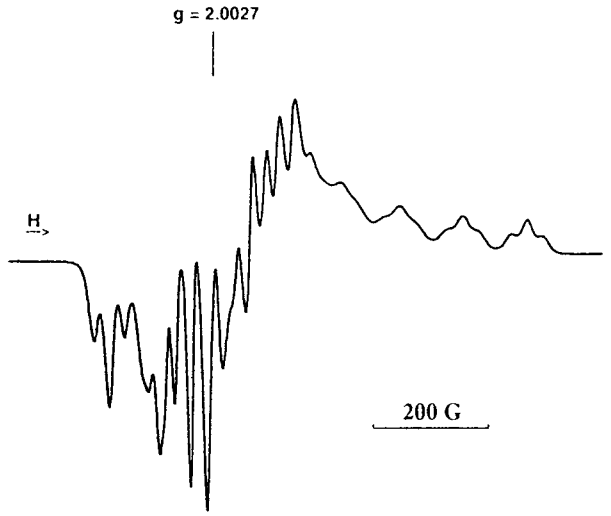

Figure 1. EPR spectrum of **1a** in toluene at −190 °C.

dmpe chemical shifts as $Mn(dmpe)_2(C{\equiv}CR')_2$ derivatives,[16] but the signals of the former species are broader ($w_{1/2}(CH_3) \approx 3370$ Hz (**1a**) and 1130 Hz (**2a**)). Analogously, the range of the chemical shifts of the dmpe signals of the cationic derivatives $[\mathbf{1a}]^+$ and $[\mathbf{2a}]^+$ are close to those of the bis(alkynyl) cations $[Mn(dmpe)_2(C{\equiv}CR')_2]^+$.[16] These findings indicate low-spin states for both the neutral and the cationic derivatives in solution.

The low-spin character of **1a** and **2a** is confirmed by their X-band EPR spectra. The solution EPR spectra show broad singlets centered near $g = 2$ at temperatures above −100 °C. At liquid-nitrogen temperature toluene glasses of both complexes give well-resolved and similar EPR spectra. Figure 1 shows the EPR spectrum of **1a** in toluene at −190 °C. The parallel features (1:2:1 triplets) at the low- and high-field ends can be separated from the perpendicular ones in the center: $g_\perp = 2.07$, $g_\parallel = 2.19$, $A(^{55}Mn, I = {}^5/_2) = 100$ G and $A(^{31}P, I = {}^1/_2) = 25$ G. These spectra are qualitatively similar to those of other low-spin Mn(II) half-sandwich complexes[27] and different from those recorded for high-spin compounds.[26] The corresponding cationic Mn(III) complexes $[\mathbf{1a}]^+$ and $[\mathbf{2a}]^+$ are EPR-silent.

Syntheses of Bis(alkynyl)bis(dmpe)manganese Complexes $Mn(dmpe)_2(C{\equiv}CR')_2$ ($R' = Ph$, $SiMe_3$; 3, 4). Bis(alkynyl)bis(dmpe)manganese complexes **3** and **4** can be obtained from manganocene/acetylene/dmpe reaction mixtures. For optimal yields it proved necessary to apply the stoichiometric 1:2:2 ratio of the starting components (Scheme 1). **3** and **4** thus generated from manganocenes are spectroscopically and analytically identical with those isolated from the reaction of $Mn(dmpe)_2Br_2$ with lithiated acetylenes.[16] In the absence of dmpe and acetylene the pure complexes **1a** and **2a** tend to equilibrate with the bis(alkynyl)bis(dmpe)-manganese species **3** and **4** and the corresponding manganocene (Scheme 2). The final equilibrium—as measured by ^1H NMR spectroscopy in C_6D_6—is reached within several days (**1a**, **1a**:**3** ≈ 1:6, 12 days; **2a**, **2a**:**4** ≈ 1:7, 10 days).

Radical Reactions of 1a/2a and $[1a]^+$/$[2a]^+$: Synthesis of the Vinylidene Complexes 5 and 6 and the Binuclear Complexes 7 and 8. The complexes **1a** and **2a** are labile and show a great tendency to undergo carbon-centered radical reactions as hydrogen abstraction or radical coupling. Both routes are competitive, producing the mononuclear vinylidene complexes **5** and **6** or the binuclear bis(vinylidene) derivative **7** (Scheme 3).

Scheme 2. Equilibrium between 1, 2 and 3, 4

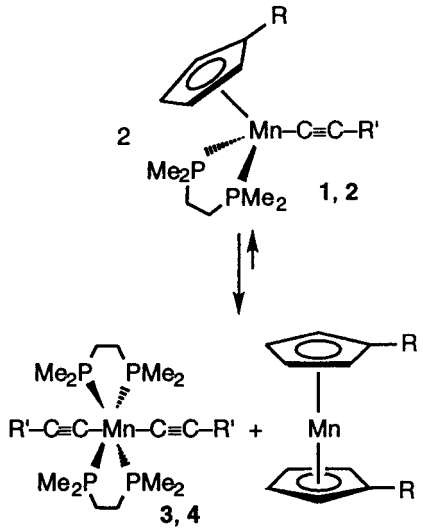

The course of these transformations depends strongly on the nature of R′ and the solvent, i.e., the ability of any of the components to donate a hydrogen radical. For the trimethylsilyl derivatives ($R' = SiMe_3$) dimerization with C−C coupling comparable to the formation of **7** does not occur, which is presumably due to steric shielding of the radical centers. Instead, complex **6** is formed by hydrogen abstraction (Scheme 3). To probe the role of the solvent as a $H^\bullet$ source, this reaction was carried out in C_6D_6. Prolonged stirring of **2a** in C_6D_6 results in the formation of nondeuterated **6** so that the hydrogen atoms must originate from R′, MeC_5H_4, or the phosphine moieties. For the phenyl derivative **1a** both pathways of Scheme 3 are available, giving a mixture of the complexes **5** and **7**.

When **1a** or **2a** is reacted with *n*-Bu_3SnH as $H^\bullet$ source, the $H^\bullet$ scavenging products are formed in 83% (**5**) and 43% (**6**) yields, respectively (Scheme 4a). As byproducts the $SnBu_3$-substituted vinylidene complexes $(MeC_5H_4)Mn(dmpe)(=C=C(R')SnBu_3)$ have been identified spectroscopically. A complete separation of these complexes from the species **5** or **6** could not be achieved, neither by fractional crystallization nor by chromatography. To circumvent this byproduct formation, $(C_5Me_5)Mo(CO)_3H$ is applied as $H^\bullet$ source (Scheme 4b). In this case **1** and **2** are quantitatively and cleanly converted to **5** and **6**, respectively. This chemical selectivity may be due to the known high recombination rate of $[(C_5Me_5)Mo(CO)_3]^\bullet$ radicals.[28] The complexes **5** and **6** may also be prepared by reaction of $(MeC_5H_4)Mn(\eta^6\text{-}C_7H_8)$ with phosphines and terminal alkynes.[29]

5 and **6** can be oxidized to $[\mathbf{1a}]^+$ and $[\mathbf{2a}]^+$ by reaction with stoichiometric amounts of $[(C_5H_5)_2Fe](BF_4)$ under H_2 elimination. The cationic complexes are isolated as

(27) Pike, R. D.; Rieger, A. L.; Rieger, P. H. *J. Chem. Soc., Faraday Trans.* **1989**, *85*, 391.

(28) Hugheys, J. L.; Bock, C. R.; Meyer, T. J. *J. Am. Chem. Soc.* **1975**, *97*, 4440.

(29) Krivykh, V. V.; Berke, H. Unpublished results.

Scheme 3. Competitive Reaction of 1 and 2 To Give 5−7

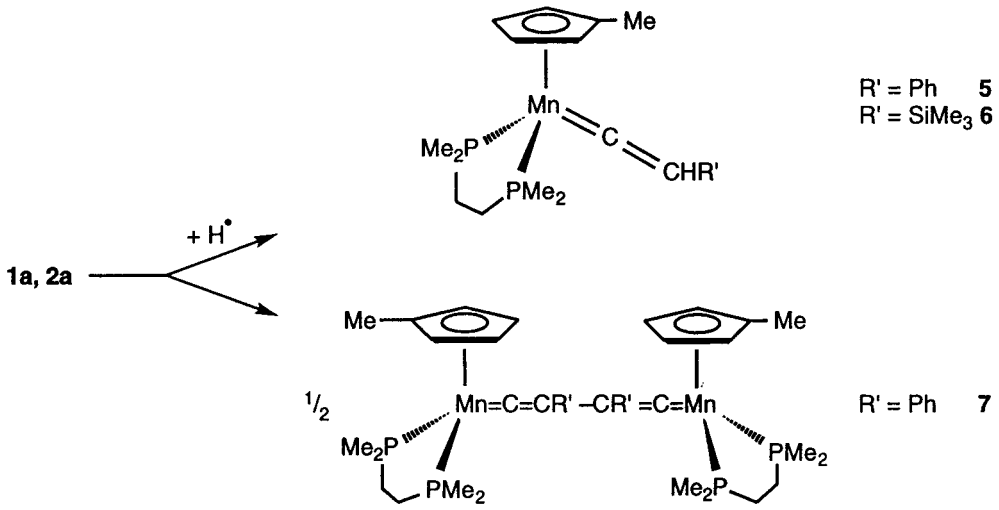

Scheme 4. Selective Reaction of 1 and 2 To Give 5 and 6

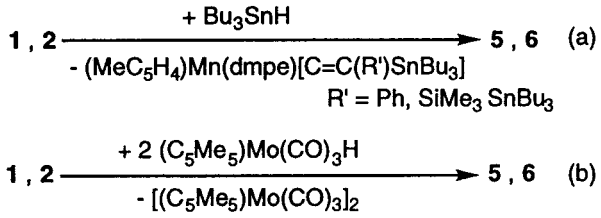

their tetrafluoroborate salts in 85% and 79% yields, respectively.

The dimeric compound **7** (Scheme 3) is obtained only in moderate yields due to the competition with the hydrogen abstraction process but can be separated from the vinylidene species **5** by fractional crystallization from pentane. **5** cannot be isolated from this mixture and is only detected spectroscopically.

The preparation of divinylidene-bridged complexes of the general formula $[L_nM{=}C{=}CR{-}CR{=}C{=}ML_n]^{m+}$ (M = Fe, Ru, Mo; R = H, Me, *n*-Bu, Ph, $SiMe_3$; m = 0, 1) was reported earlier.[30,31] All of them were formed via dimerization of odd-electron complexes generated in redox transformations. However, in situ generated or isolable radicals $[(C_5R_5)M(dppe)(C{=}C(H)R')]^+$ (M = Fe,[22] Ru;[23] R = H, Me; R′ = *t*- Bu, Ph) and $[Mo(C_7H_7)(dppe)\text{-}(C{\equiv}C\text{-}t\text{-}Bu)]^+$ [30d,e] are stable, demonstrating that the course of such radical dimerizations depends on the bulkiness of the organic substituents, the metal center, and the ancillary ligands. Besides **1a**, only one neutral complex in these coupling series is known in the literature;[30g] all other processes are based on cationic species. Obviously, the charge of the dimerizing species is not an important factor, as long as the radical character is sufficiently delocalized onto the β-carbon atom. Indeed, $[\mathbf{1a}]^+$ slowly dimerizes to give the dicationic bis(carbyne) compound **8**, which can be separated from further decomposition products by crystallization in about 20% yield (Scheme 5).

Scheme 5. Synthesis of 8 from $[1a]^+$ and Redox Reactions To Give 7

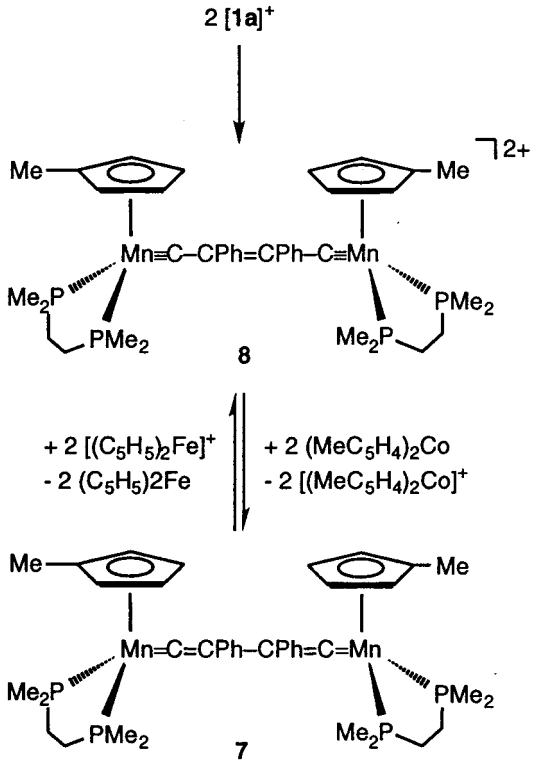

Scheme 6. Formal C−C Coupling Reaction of Cationic Mn(III) Acetylide Complexes

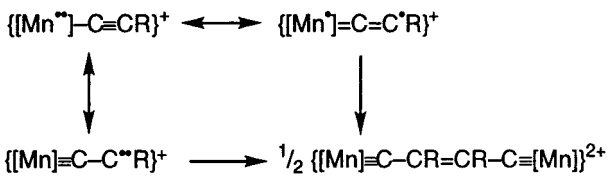

Since $[\mathbf{1a}]^+$ has to be considered a biradical, this process can be envisaged to occur by coupling of triplet carbene centers (Scheme 6). Alternatively, a formally stepwise electron pairing via carbon-centered mono-

(30) (a) Iyer, R. S.; Selegue, J. P. *J. Am. Chem. Soc.* **1987**, *109*, 910. (b) Le Narvor, N.; Lapinte, C. *J. Chem. Soc., Chem. Commun.* **1993**, 357. (c) Le Narvor, N.; Toupet, L.; Lapinte, C. *J. Am. Chem. Soc.* **1995**, *117*, 7129. (d) Beddoes, R. L.; Bitcon, C.; Ricalton, A.; Whitley, M. W. *J. Organomet. Chem.* **1989**, *367*, C21. (e) Beddoes, R. L.; Bitcon, C.; Grime, R. W.; Ricalton, A.; Whitley, M. W. *J. Chem. Soc., Dalton Trans.* **1995**, 2873. (f) Bruce, M. I.; Cifuentes, M. P.; Snow, M. R.; Tiekink, R. T. *J. Organomet. Chem.* **1989**, *359*, 379. (g) Löwe, C.; Hund, H.-U.; Berke, H. *J. Organomet. Chem.* **1989**, *372*, 295.

(31) Bruce, M. I. *Chem. Rev.* **1991**, *91*, 213.

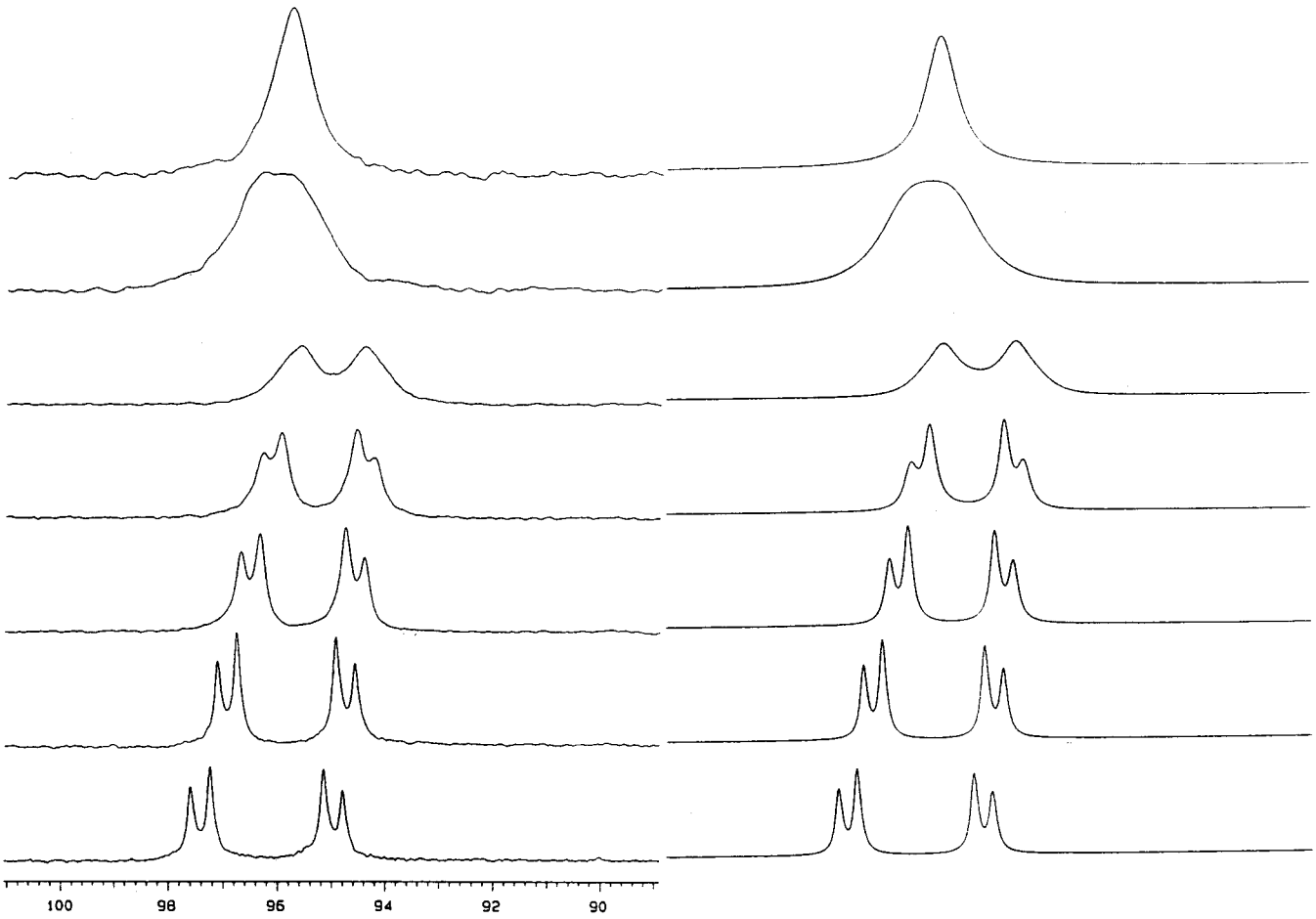

Figure 2. Variable-temperature ^{31}P NMR spectra of **7** (at −70, −50, −30, −10, 10, 22, and 45 °C) and simulated spectra.

radicals as suggested in Scheme 6 could serve as a model. Such coupling reactions of 16-VE complexes have not been observed previously, but the principal structural type of such species, binuclear complexes containing a bis(carbyne) bridging unit, have already been reported.[32] **8** can also be prepared in quantitative yield by oxidation of **7** with 2 equiv of a ferrocenium salt (Scheme 5). Rereduction can be accomplished by reaction of **8** with methylcobaltocene (Scheme 5). Both compounds **7** and **8** are thermally stable, and complex **8** is even air-stable. The IR spectrum of **7** shows two medium-strong bands at 1562 and 1589 cm^{-1} in the characteristic range for vinylidene ligands (but an assignment is difficult due to the overlap with the C=C vibrations of the phenyl rings).[31] **8** additionally possesses a broad C=C absorption band at 1632 cm^{-1}.

In the ^{13}C NMR spectrum of **5** the resonance for the C_α atom appears as a triplet at 342.6 ppm ($^2J_{PC}$ = 35 Hz) substantially upfield from those of $(MeC_5H_4)MnL_2(C{=}CPh_2)$ (L = CO, 395.7 ppm; L = $PPhMe_2$, 381.4 ppm[33]). For comparison, the corresponding C_α resonances in carbyne complexes $[(C_5H_5)MnLL'(\equiv CPh)]^+$ appear at 356.9 (L = L′ = CO[34]) and 343.7 (L = CO, L′ = PPh_3[35]). Obviously the C_α resonances in these complexes shift to higher field strength upon substitution of CO by phosphines.

The $^{31}P\{^1H\}$ NMR spectrum of **8** displays a sharp, temperature-independent singlet at 83.2 ppm, while for **7** the signal of the phosphorus nuclei at 95.6 ppm is broadened at room temperature. At 203 K the spectrum exhibits an AB quartet at 93.4 ppm (J_{PP} = 42.3 Hz). When the temperature is raised, the components of the AB system broaden and coalesce at 295 K ($\Delta\nu$ = 246.5 Hz). By line shape analysis of the ^{31}P NMR spectra of **7** at different temperatures the free energy of activation, $\Delta G^{\ddagger}$, is evaluated as 56.7 kJ mol^{-1} for the two-site exchange process (Figure 2). This barrier is attributed to the hindered rotation around the Mn=C bond, and it is significantly higher than the barriers in the mononuclear complex **5** ($\Delta G^{\ddagger}$ = 36.0 kJ mol^{-1}),[29] in $[(C_5H_5)M(L{-}L)(=CHR)]^+$ species (R = H, Ph, M = Fe, L−L = dppm, 41.0 kJ mol^{-1} [36] and L−L = dppe, 39.3 kJ mol^{-1};[37] M = Ru, L−L = dppe, 38.1 kJ mol^{-1} [38]) and even in the binuclear compound $[(C_5H_5)_2Fe_2(dppe)_2(\mu\text{-}C_4Me_2)]^{2+}$ (37 kJ mol^{-1}).[30a]

For the iron and ruthenium complexes the horizontal vinylidene ligand orientation (the $C{=}CR_2$ vinylidene

(32) (a) Ustynyuk, N. A.; Vinogradova, N. V.; Andrianov, V. G.; Stuchkov, Y. T. *J. Organomet. Chem.* **1984**, *268*, 73. (b) Krouse, S. A.; Schrock, R. R. *J. Organomet. Chem.* **1988**, *355*, 257. (c) Shih, K.-Y.; Schrock, R. R.; Kempe, R. *J. Am. Chem. Soc.* **1994**, *116*, 8804. (d) Woodworth, B. E.; White, P. S.; Templeton, J. L. *J. Am. Chem. Soc.* **1997**, *119*, 828.

(33) Schubert, U.; Grönen, J. *Chem. Ber.* **1989**, *122*, 1237.

(34) Fischer, E. O.; Meineke, E. W.; Kreissl, F. R. *Chem. Ber.* **1977**, *110*, 1140.

(35) Terry, M. R.; Kelley, C.; Lugan, N.; Geoffrey, G. L.; Haggarty, B. S.; Rheingold, A. L. *Organometallics* **1993**, *12*, 3607.

(36) Gamasa, M. P.; Gimeno, J.; Lastra, E.; Martin, B. M.; Anillo, A.; Tiripicchio, A. *Organometallics* **1992**, *11*, 1373.

(37) Consiglio, G.; Bangerter, F.; Darpin, C.; Morandini, F.; Lucchini, V. *Organometallics* **1984**, *3*, 1446.

(38) Consiglio, G.; Morandini, F. *Inorg. Chim. Acta* **1987**, *127*, 79.

plane is perpendicular to the pseudo mirror plane bisecting the $(C_5H_5)ML_2$ moiety) was predicted theoretically[39] and proven by crystallographic investigations.[36,40] Recently, the first examples of vertical orientations of vinylidene ligands were reported for the mono- and binuclear complexes $[Mo(C_7H_7)(dppe)(=C=CHPh)]^+$ and $[(Mo_2(C_7H_7)_2(dppe)_2(\mu\text{-}C_4Ph_2)]^{2+}$.[30e]

From variable-temperature ^1H, ^{13}C, and ^{31}P NMR spectra it can be deduced that the preferred orientation of the vinylidene ligands in **5** and **7** is horizontal, as all signals of **5** and **7** (α, α', β, β' of the cyclopentadienyl ring (H, C); *o*-, *m*-H or *o*-, *m*-C of the phenyl ring and other pairs of nuclei) are separated at low temperature but coincide for both fragments of **7** at elevated temperature. These observations confirm that the frozen rotation of the vinylidene unit gives rise to signals of two isomers containing diastereotopic H, C, and P nuclei. The binuclear bis(vinylidene) complex **7** is expected to have free or almost free rotation around the central C−C bond, causing no isomerism based on this motion.

X-ray Diffraction Studies on 2a, 5, 7 and 8. Compounds **2a** and **5** were subjected to X-ray structural analyses, because **2a** is a rare example of an organometallic acetylide system with d^5 low-spin configuration and it seemed to be intriguing to compare **2a** with the related electronically saturated vinylidene complex **5**. Significant structural changes might arise, as **2a** is one hydrogen atom deficient with respect to **5**. The structures (Figure 3, Table 1) are compared on the basis that the replacement of a trimethylsilyl group (**2a**) by a phenyl substituent (**5**) has only a minor influence.

The geometry around the manganese center in **2a** is pseudotetrahedral, which compares favorably with those of related vinylidene complexes[42] and also with compound **5**. The formal abstraction of $H^\bullet$ or $R^\bullet$ from a vinylidene ligand does not give rise to severe structural reorganization with respect to the P−Mn−P, P−Mn−C, Cp′−Mn−C, and Cp′−Mn−P angles[41] (Table 1). The Mn−C1 distance in **2a** is approximately 0.2 Å larger than that of **5** (Table 1), indicating that the vinylidene moiety is a strong π-accepting ligand, while the acetylide group of **2a** behaves π-saturated in its interaction with the metal center. This is also supported by the smaller C−C distance of **2a**, with triple-bond character, compared to that of **5**, exhibiting double-bond character (Table 1). The complexes **2a** and **5** are therefore well-represented by the valence bond structures presented in Schemes 1 and 3.

The molecular structures of **7** and **8** are illustrated in Figure 4; selected bond lengths and angles are given in Table 2. The binuclear complex **7** contains no center of symmetry similar to the structure of the related dimer $[(C_5H_5)_2Fe_2(dppe)_2(\mu\text{-}C_4Me_2)](BF_4)_2$,[30a] however, in contrast to the centrosymmetric dimer $[Mo_2(C_7H_7)_2(dppe)_2(\mu\text{-}C_4Ph_2)](PF_6)_2$.[30d,e] The orientation of the vinylidene ligand in both fragments is almost horizontal: the angle between the plane through Cp1−Mn1−C1 [41] and the

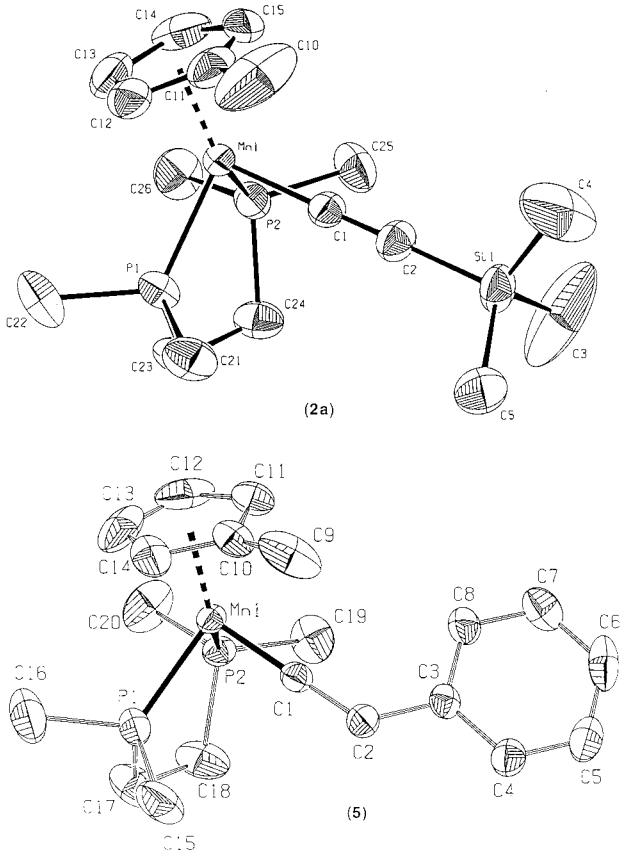

Figure 3. X-ray structures of **2a** and **5**.

Table 1. Selected Bond Distances (Å) and Angles (deg) for Complexes 2a and 5[41]

	2a	5
Mn−P1	2.2118(9)	2.204(2)
Mn−P2	2.212(1)	2.191(2)
Mn−C1	1.921(3)	1.731(5)
C1−C2	1.226(4)	1.344(6)
Mn−Cp	1.78(1)	1.79(1)
P1−Mn−P2	83.22(3)	84.01(6)
P1−Mn−C1	89.78(8)	90.9(2)
P2−Mn−C1	87.2(1)	88.7(2)
Mn−C1−C2	179.4(3)	178.2(5)
P1−Mn−Cp	127.4(4)	124.81(6)
P2−Mn−Cp	128.7(3)	128.93(6)
C1−Mn−Cp	126.2(4)	126.4(4)

vinylidene plane through C1−C2−C3 amounts to 74°, and that between the plane through Cp2−Mn31−C31[41] and the plane through C31−C32−C33 amounts to 79°. In the iron dimer the corresponding angles are 90 and 117°,[30a] while in the molybdenum dimer the ligand orientation approximates that of a vertical one with a 19° tilt.[30d,e] The C1−C2−C32−C31 torsional angle is 273.6(5)°, in contrast to a planar s-trans conformation at the central C−C bond found in the iron and molybdenum dimers (torsional angle 0°). The phenyl rings are only slightly rotated (16.8(4)°) from their ideal coplanar position, allowing conjugation with the double bonds of the vinylidene ligands. This leads to a shortening of the C−C distances between the phenyl groups and the vinylidene backbone and concomitantly to an increase of the central C2−C32 bond length (Table 2) compared to that in the molybdenum dimer with a planar bridging carbon unit and almost perpendicular phenyl rings. Other structural parameters of the Mn−C_4−Mn bis-

(39) (a) Schilling, B. E. R.; Hoffmann, R.; Lichtenberger, D. L. *J. Am. Chem. Soc.* **1979**, *101*, 585. (b) Kostic, N. M.; Fenske, R. F. *Organometallics* **1982**, *1*, 974.

(40) Miller, D. C.; Angelici, R. J. *Organometallics* **1991**, *10*, 79.

(41) Cp denotes the centroid of the cyclopentadienyl or methylcyclopentadienyl ring.

(42) Bruce, M. I.; Swincer, A. G. *Adv. Organomet. Chem.* **1983**, *22*, 59.

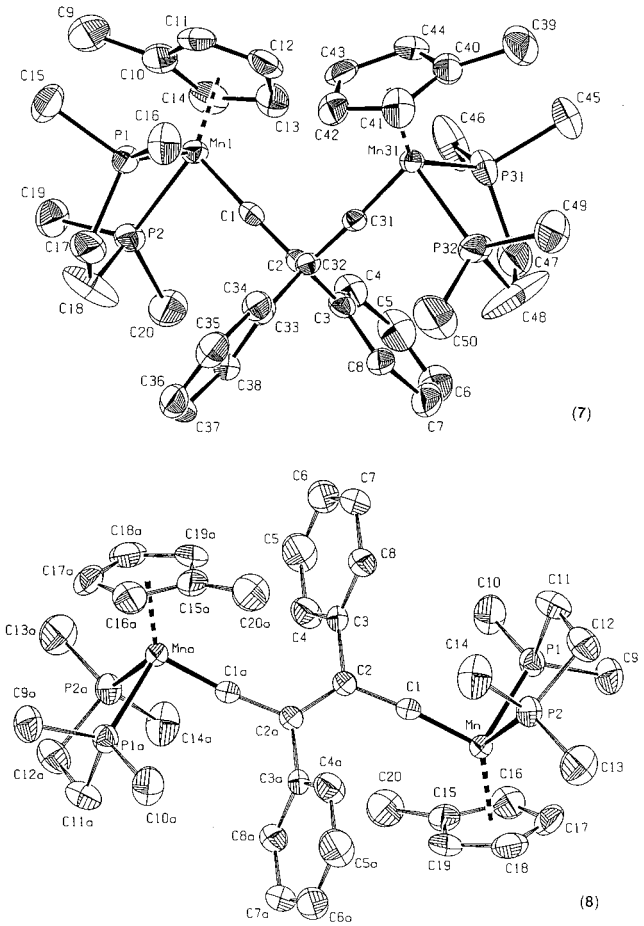

Figure 4. X-ray structures of **7** and **8**.

Table 2. Selected Bond Distances (Å) and Angles (deg) for Complexes 7 and 8[41]

	7	8
Mn1−P1	2.188(2)	2.250(1)
Mn1−P2	2.190(2)	2.275(1)
Mn1−C1	1.742(5)	1.684(3)
Mn1−Cp1	1.79(2)	1.79(2)
C1−C2	1.351(6)	1.421(5)
C2−C3(Ph)	1.471(6)	1.486(5)
C2−C32	1.529(6)	1.400(7)
Mn31−P31	2.182(2)	
Mn31−P32	2.183(2)	
Mn31−C31	1.737(4)	
Mn31−Cp31	1.79(2)	
C31−C32	1.353(6)	
C32−C33(Ph)	1.478(6)	
P1−Mn1−P2	83.28(6)	84.47(5)
P1−Mn1−C1	91.5(2)	97.1(1)
P2−Mn1−C1	88.6(2)	97.1(1)
P1−Mn1−Cp1	125.6(7)	119.7(5)
P2−Mn1−Cp1	130.1(7)	123.8(5)
C1−Mn1−Cp1	124.8(9)	125.1(7)
Mn1−C1−C2	177.4(4)	169.7(3)
P31−Mn31−P32	82.92(7)	
P31−Mn31−C31	90.7(1)	
P32−Mn31−C31	89.4(2)	
P31−Mn31−Cp31	125.1(8)	
P32−Mn31−Cp31	130.1(7)	
C31−Mn31−Cp31	125.4(9)	
Mn31−C31−C32	177.4(4)	

(vinylidene) moiety such as Mn=C and C=C distances and Mn=C=C angles (Table 2) fall in a typical range.[31,42]

The dicationic complex **8** possesses crystallographic inversion symmetry, giving rise to a trans conformation

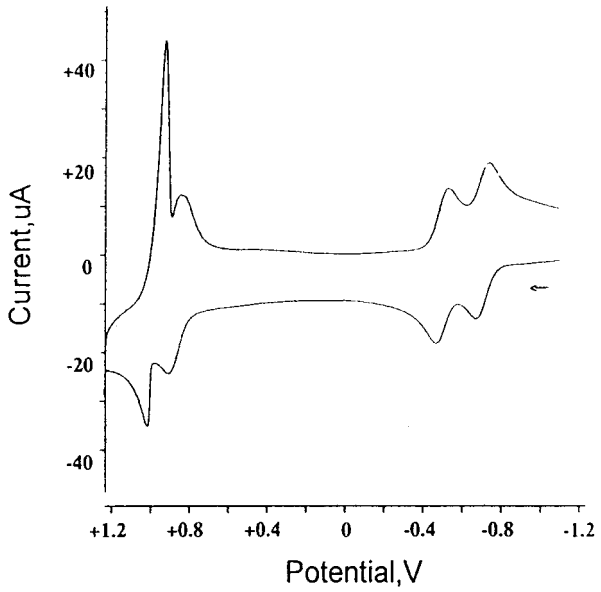

Figure 5. Cyclic voltammogram of **7** (10^{-3} M in 0.1 M n-Bu_4NPF_6/CH_2Cl_2; vs Fc/Fc^+; 0.4 V s^{-1}).

about the olefinic bridge. The Mn1−C1−C2−C2a−C1a−Mn1a backbone forms a plane including the C3 and C3a ipso carbon atoms of the phenyl substituents. The phenyl rings are rotated by 68.2(2)° out of conjugation with respect to the plane of the conjugated system. The C2=C2a distance (Table 2) is slightly larger than that of the related dimer $(C_5H_5)_2Cr_2(CO)_4(\mu$-$C_4Ph_2)$ (C=C = 1.375 Å[32a]) and is significantly elongated compared to that of (vinylcarbyne)manganese complexes $[(C_5H_5)Mn(CO)_2(\equiv CCH{=}CPh_2)]^+$ (C=C = 1.357 Å[43]), $[(C_5H_5)Mn(CO)(PPh_3)(\equiv CCMe{=}CPh_2)]^+$ (C=C = 1.357 Å[35]), the methyl-substituted dimer $Tp'_2W_2(CO)_4(\mu$-$C_4Me_2)$ (Tp′ = hydridotris(3,5-dimethypyrazolyl)borate; C=C = 1.36 Å[32d]), and typical isolated (C=C = 1.299 Å) and conjugated (C=C = 1.330 Å) double bonds in organic molecules.[44] This might be the result of enhanced crowding, which is maximal in the binuclear derivative **8**. The lengthening of the Mn≡C distance compared to that in (vinylcarbyne)manganese complexes (1.665−1.668 Å[35,43]) is only marginal.

Cyclic Voltammetry, Near-IR, and EPR Investigations on the 7/8 Redox Couple. As the complexes **7** and **8** can be reversibly converted by redox reagents, we have studied the redox properties of **7** in more detail, applying cyclic voltammetry (Figure 5). Two fully reversible redox couples are found at $E_{1/2} = -0.656$ and −0.445 V vs Fc/Fc^+ ($\Delta E_p = 0.060-0.065$ V and $i_{pa}/i_{pc} \approx 1$ for scan rates of 0.050−0.500 V s^{-1}). The separation of these waves amounts to 0.211 V, consistent with two successive one-electron-oxidation steps, yielding the monocation $[\mathbf{7}]^+$ and the dication **8**, respectively (Scheme 7).

Another pair of waves is observed at about 1.5 V higher potentials, which can be assigned to the next oxidation steps producing Mn(IV) derivatives. The first wave ($E_{1/2} = 0.945$ V; $\Delta E_p = 0.065$ V) is reversible at high scan rates, but at values lower than 0.400 V s^{-1}

(43) Kolobova, N. E.; Ivanov, L. L.; Zhvanko, O. S.; Khitrova, O. M.; Batsanov, A. S.; Struchkov, Y. T. *J. Organomet. Chem.* **1984**, *262*, 39.
(44) Allen, F. H.; Kennard, O.; Watson, D. G.; Brammer, L.; Orpen, G.; Taylor, R. *J. Chem. Soc., Perkin Trans.* 2 **1981**, S1.

Scheme 7. Redox Transformation of 7, [7]$^+$, and 8

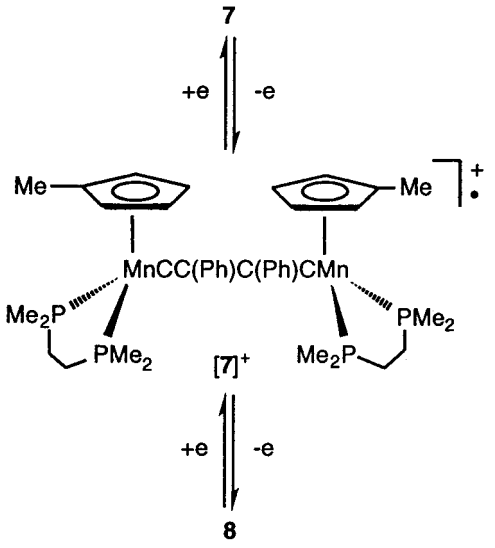

the intensity of the cathodic peak grows to give $i_{pa}/i_{pc} < 1$. A similar situation exists for the wave at $E_{p1} = 1.088$ V, $E_{p2} = 0.993$ V ($\Delta E_p = 0.095$ V) at all scan rates applied. These cathodic stripping peaks show that the Mn(IV) derivatives precipitate on the working electrode. The formal separation of these waves is less than in the previous case ($\Delta E = 0.096$ V). The magnitude of separations between formal redox potentials of binuclear complexes is an indication of the strength of the electronic interactions between the metal centers and therefore is an important characteristic of the electronic conductivity of the bridges.[45] From the separation between two one-electron steps the comproportionation constant[46] $K_{c1} = 8 \times 10^3$ can be derived for the equilibrium $[Mn_2]^0 + [Mn_2]^{2+} \rightleftarrows 2[Mn_2]^+$ and $K_{c2} = 77$ (albeit thermodynamically not strictly correct, as the redox processes are not reversible) for the equilibrium $[Mn_2]^{2+} + [Mn_2]^{4+} \rightleftarrows 2[Mn_2]^{3+}$. The former value suggests a class II or class III behavior in the Robin−Day nomenclature[47] for the monocationic mixed-valence complex [**7**]$^+$; the latter shows that the mixed-valence tricationic complex is only weakly coupled and is less stable toward disproportionation.

The mixed-valence compound [**7**]$^+$ can be prepared by oxidation of **7** (red) with 1 equiv of $[(C_5H_5)_2Fe](BF_4)$, by reduction of **8** (orange) with 1 equiv of $(MeC_5H_4)_2Co$, or by comproportionation of equimolar amounts of **7** and **8**. The resulting red-green solution has been analyzed by EPR and near-IR spectroscopy. The EPR spectrum (Figure 6) measured in a dichloromethane matrix at −190 °C shows an undecet with broad individual lines ($g \approx 2.018$, $A(^{55}Mn) = 60$ G). This pattern and the small hyperfine coupling to the Mn centers (approximately half of that of the mononuclear complexes **1a** and **2a** and of other mononuclear low-spin manganese compounds[16,27]) points to an electron delocalization over both Mn centers or a very rapid electron transfer (time scale of the EPR method: 10^8 s^{-1}).

The near-IR spectrum of [**7**]$^+$ shows an asymmetric intense absorption band ($\lambda = 1018$ nm; $\epsilon = 3.3 \times 10^3$ M^{-1}cm^{-1}; $\nu_{1/2} \approx 3120$ cm^{-1}; shoulder at ∼900 nm) in a spectral range in which **7** and **8** are transparent (Figure 7). The bandwidth at half-height is smaller than expected from Hush's theory[48] for weakly coupled mixed-valence compounds ($\nu_{1/2} \approx 4765$ cm^{-1}) and is therefore better assigned a transition between delocalized states rather than an intervalence transition. This is in accord with the conclusion drawn from the EPR measurement and also conforms with the thermodynamic stability of [**7**]$^+$ as determined from the CV measurement. The observed splitting of this absorption band into at least two components might be due to mixing with other excited charge-transfer states, but a definitve assignment is impossible at the moment.

Figure 6. EPR spectrum of **1a** in dichloromethane at −190 °C.

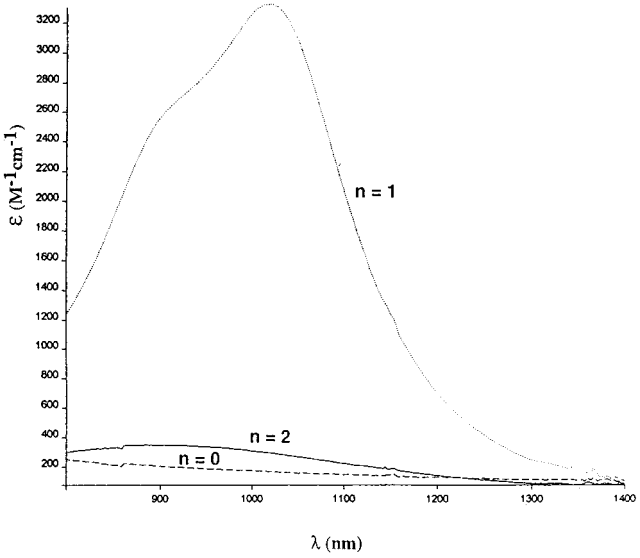

Figure 7. Near-IR spectra of **7**, [**7**]$^+$, and **8** in dichloromethane.

DFT Calculations on 7, [7]$^+$, and 8. We have perfomed density functional calculations on the compounds $[\{(C_5H_5)Mn(PH_3)_2\}_2(\mu\text{-}C_4H_2)]^{n+}$ ($n = 0-2$; Scheme 8) modeling the complexes $[\{(MeC_5H_4)Mn(dmpe)\}_2(\mu\text{-}C_4Ph_2)]^{n+}$ ($n = 0$, **7**;, $n = 1$, [**7**]$^+$; $n = 2$, **8**).

The ground states, configurations, and energies of the binuclear systems are given in Table 3 and the main

(45) Seyler, J. W.; Weng, W.; Zhow, Y.; Gladysz, J. A. *Organometallics* **1993**, *12*, 3802.
(46) Creutz, C. *Prog. Inorg. Chem.* **1983**, *30*, 1.
(47) Robin, M. B.; Day, P. *Adv. Inorg. Chem. Radiochem.* **1967**, *10*, 247.
(48) (a) Hush, N. S.; *Prog. Inorg. Chem.* **1967**, *8*, 391. (b) Hush, N. S. *Coord. Chem. Rev.* **1985**, *64*, 135.

Scheme 8. Binuclear Model Complexes

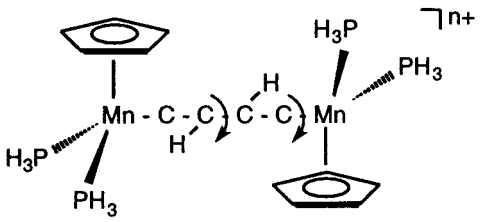

Table 3. Electronic States, Complex Configurations, and Energies (with Respect to Atoms) for the Model Complexes $[\{(C_5H_5)Mn(PH_3)_2\}_2(\mu\text{-}C_4H_2)]^{n+}$ ($n = 0-2$)

n	state	complex confign	energy/eV
0	^{1}A	$(64a)^2(65a)^2$	−243.08
1	^{2}A	$(64a)^2(65a)^1$	−238.14
2	^{1}A	$(64a)^2(65a)^0$	−229.45

Table 4. Main Optimized Geometrical Parameters[a] of $[\{(C_5H_5)Mn(PH_3)_2\}_2(\mu\text{-}C_4H_2)]^{n+}$ ($n = 0-2$)[b]

	$n = 0$	$n = 1$	$n = 2$
$Mn-P^1$	2.198/2.201	2.233/2.232	2.271/2.267
$Mn-P^2$	2.200/2.197	2.232/2.233	2.268/2.270
$Mn-C^1$	1.749/1.750	1.694/1.694	1.650/1.649
C^1-C^3	1.322/1.322	1.358/1.359	1.394/1.394
C^3-C^4	1.465	1.422	1.375
P^1-Mn-P^2	91.3/91.4	93.1/93.1	94.0/94.1
P^1-Mn-C^1	90.4/90.1	91.2/91.3	93.0/93.5
P^2-Mn-C^1	90.1/89.7	91.3/91.2	93.6/92.9
$Mn-C^1-C^3$	179.3/178.2	179.1/179.0	179.2/179.3
$C^1-C^3-C^4$	125.3/126.3	124.2/124.2	122.5/122.5
$C^1-C^3-C^4-C^2$	181.4	179.9	180.1

[a] Distances in Å and angles in deg. [b] The first number refers to the Mn^1 moiety and the second to the Mn^2 fragment.

geometrical parameters in Table 4. The general electronic features of the metal fragment $\{(C_5H_5)Mn(PH_3)_2\}$ as well as the bonding to vinylidene fragments $\{:C{=}CH_2\}$ in mononuclear complexes were described earlier. [39b] Our calculations are in full agreement with these results; therefore, our description of the bonding will be restricted to those points essential for the binuclear situation. The important four metal fragment orbitals ($\pi_v-\sigma$; Scheme 9, Table S1 of the Supporting Information) are mainly localized on the metal center and are essentially composed of its 3d orbitals. The π_v orbitals can π-donate in the vertical (yz) plane, whereas the HOMO π_h can π-donate in the horizontal (xy) plane. The ligand fragment $\{:C^1{=}C^3(H)C^4(H){=}C^2:\}$ may be viewed as containing sp- (C^1 and C^2) and sp^2-hybridized carbon atoms (C^3 and C^4) with double bonds between C^1/C^3 and C^2/C,[4] respectively. Its important orbitals (Scheme 9, Table S2 of the Supporting Information) are the π bonding orbitals ($1\pi_u$ and $1\pi_g$), the vacant π type p orbitals of the ligating carbon atoms C^1 and C^2 ($1p_u$ and $1p_g$), the π antibonding orbitals ($2\pi_u$ and $2\pi_g$), and the σ type sp orbitals ($1\sigma_u$ and $1\sigma_g$).

The electronic interaction between the C_4H_2 bridging unit and the metal fragments will be discussed by considering a fragment approach in which two $\{(C_5H_5)Mn(PH_3)_2\}$ fragments interact with a C_4H_2 species (Table S3 of the Supporting Information). Scheme 9 shows the orbital interaction diagram of $[\{(C_5H_5)Mn(PH_3)_2\}_2(\mu\text{-}C_4H_2)]^0$. The interaction between the metal fragments and the bridging ligand can be divided into three groups: (i) two low-lying orbitals describing the M−C σ-bonds, formed by the in- and out-of-phase d_σ orbitals of the metal fragments interacting with the sp hybrid orbitals of the terminal carbon atoms ($1\sigma_u$ and $1\sigma_g$), (ii) levels originating from the interactions of the π donor orbitals ($1\pi_u$ and $1\pi_g$) of the ligand with the π_v combinations forming the M−C π-bonds, and (iii) orbitals composed of the π acceptor orbitals ($1p_u$ and $1p_g$) of the ligand and the appropriate combinations of two π_h metal fragment orbitals with metal−vinylidene π back-bonding character. π back-bonding is much stronger into the $1p_u$ and $1p_g$ orbitals of the ligand than into the $2\pi_u$ or $2\pi_g$ antibonding orbitals, an observation which has already been made for mononuclear $(C_5H_5)ML_2(CCH_2)$ complexes.[39b]

The multiplicity of the Mn−C bonds is between 2 and 3, allowing for a facilitated rotation around this bond (Scheme 8). The calculated energy difference between horizontal and vertical conformations amounts to 49 kJ mol^{-1} for the neutral binuclear model complex, with the horizontal orientation of the vinylidene unit being more stable. The preference of the horizontal position has already been predicted by calculations on mononuclear $(C_5H_5)ML_2(CCH_2)$ complexes[39b] and confirmed by X-ray structural analyses. The energy difference between these binuclear conformers is about twice as large as that calculated for the corresponding mononuclear complex $(C_5H_5)Mn(PH_3)_2(CCH_2)$ (24 kJ mol^{-1}), in good agreement with the trend of the activation barriers observed experimentally (vide supra).

The solid-state structure of **7**, especially the torsional angle of the C_4 backbone (Scheme 8), deserves further comment. A conformational analysis of a rotation around the central C^3-C^4 bond shows an energy minimum at a torsional angle of 181.4° for the conformers in which the $\{(C_5H_5)Mn(PH_3)_2\}$ fragments are approximately related by an inversion center in the 180° conformer (Scheme 10, upper graph, conformers A; Table S4 of the Supporting Information). Rotation of one $\{(C_5H_5)Mn(PH_3)_2\}$ fragment around the Mn−C bond by 180° gives a conformer in which the $\{(C_5H_5)Mn(PH_3)_2\}$ fragments are related by a mirror plane in the 180° conformer (Scheme 10, lower graph, conformers B; Table S4 of the Supporting Information). In the conformers of the B series the 137 and 219° torsion angles are energetically favored over the 180° torsion angle by some 17 kJ mol^{-1}. The absolute minimum, however, corresponds to the A conformer with a 180° torsion angle. To answer the question whether this discrepancy with the experimental structure (approximately conformer B with a 273.6° torsional angle, vide supra) arises from electronic, steric, or crystal-packing forces, we investigated first the interaction of the phenyl rings attached to the C_4 chain with the C=C double bonds of the bridging ligand. Calculations on the two conformations of $H_2C{=}C(Ph)C(Ph){=}CH_2$ show that the twisted chain with coplanar phenyl groups, which should allow conjugation of the phenyl groups with the double bonds of the vinylidene ligand, is destabilized by 11 kJ mol^{-1} compared to the planar C_4 chain with orthogonal phenyl groups (Table S4 of the Supporting Information). Therefore, electronic reasons can be excluded. Explicit DFT calculations on the two complex conformers, including the phenyl rings $[\{(C_5H_5)Mn(PH_3)_2\}_2(\mu\text{-}C_4Ph_2)]^0$, have been carried out which show that indeed the C_4 chain twisted structure

Scheme 9. Orbital Interaction Diagram of 7

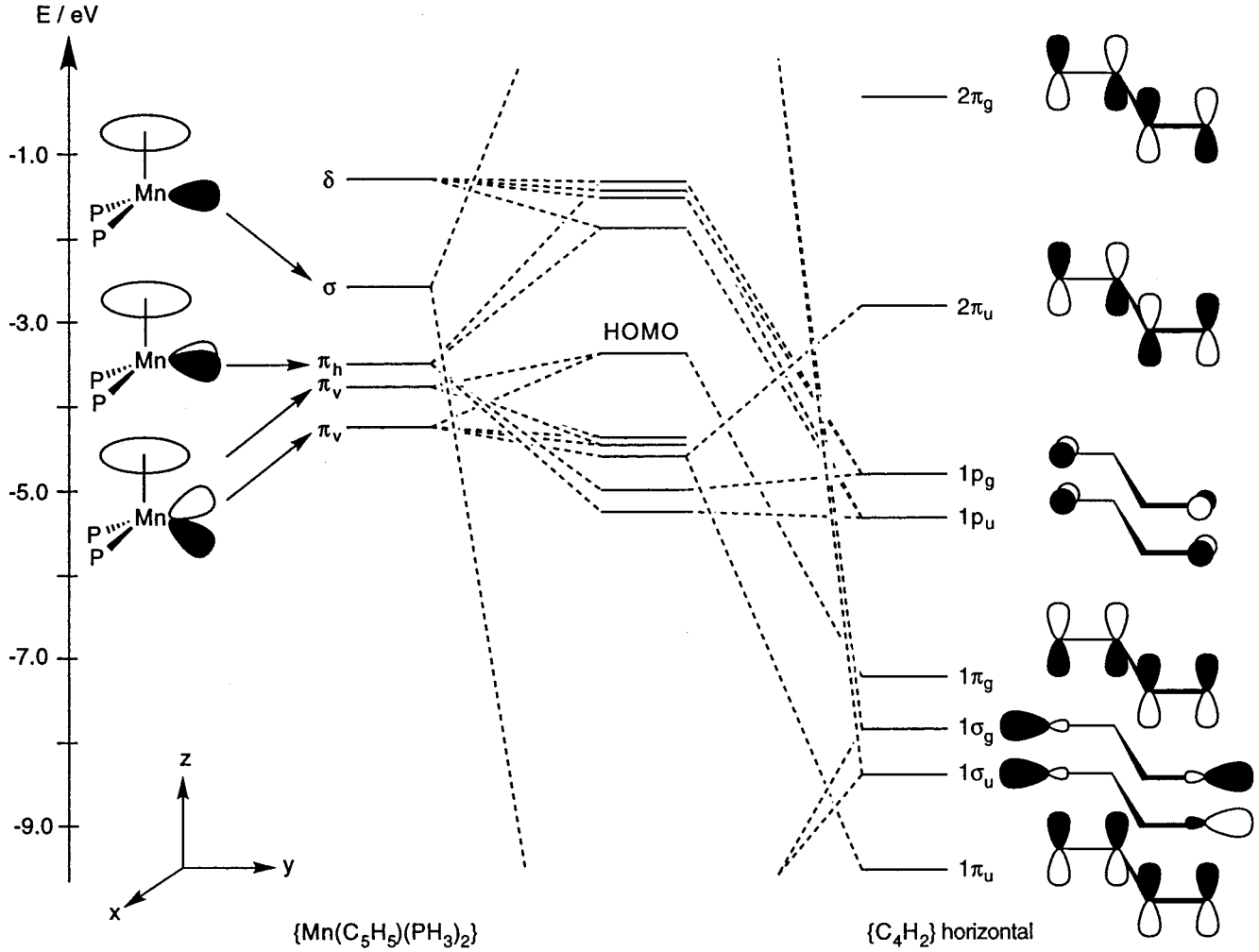

with coplanar phenyl rings is preferred over the planar C_4 backbone and orthogonal phenyl groups by 31 kJ mol^{-1} (Table S4 of the Supporting Information). Obviously, intramolecular steric crowding compensates and even surpasses the electronic preference of the planar C_4 chain and the conformation found in the solid state is neither a consequence of electronic conjugation of the phenyl groups with the vinylidene double bonds nor a crystal packing effect but an intramolecular steric effect.

For the model compounds of both oxidized complexes $[\mathbf{7}]^+$ and **8** the preferred conformation is that with a 180° $C^1C^3C^4C^2$ torsion angle, in accordance with the X-ray structural analysis for **8** (vide supra). The energetic difference between the A and B 180° isomers is small (<2 kJ mol^{-1}). Obviously, the twisting of the C_4 chain is electronically unfavorable. The interaction diagram (Scheme 9) shows that removing one or two electrons from the HOMO of the neutral complex reduces the π antibonding interaction between the central carbon atoms C^3 and C^4, resulting in an increased double-bond character which prohibits a facile rotation around this bond. In addition the π bonding interaction between C^1/C^3 and C^2/C^4 as well as the π antibonding metal ligand interaction is reduced giving rise to elongated C^1-C^3 and C^2-C^4 and shortened Mn−C bonds, respectively (Table 4). Therefore, the neutral complex is best described as a bis(vinylidene) complex and the dicationic one as a bis(carbyne) species. The calculated bond distances agree reasonably well with the experimental ones; especially the decreasing of the $Mn^{1,2}-C^{1,2}$ and the central C^3-C^4 bond lengths and the increasing of the C^1-C^3 and C^2-C^4 bond lengths on oxidizing the complex is reproduced (Tables 2 and 4). The average deviation for all Mn−L bond lengths of **7**/$[\{(C_5H_5)Mn(PH_3)_2\}_2(\mu\text{-}C_4H_2)]^0$ and **8**/$[\{(C_5H_5)Mn(PH_3)_2\}_2(\mu\text{-}C_4H_2)]^{2+}$ is less than 2%. Differences between calculated and experimental atom distances within the C_4 backbone (2−4%) might be ascribed to the steric crowding imposed by the additional phenyl groups attached to the C_4 backbone, which is corroborated by a comparison of calculated bond lengths of the stable conformer $[\{(C_5H_5)Mn(PH_3)_2\}_2(\mu\text{-}C_4Ph_2)]^0$ (Table S4 of the Supporting Information) with those of **7** (calcd/exptl C^1-C^3 1.345, 1.348/1.351, 1.353 Å; C^2-C^4 1.508/1.529 Å).

Broken-symmetry calculations on the model complex $[\{(C_5H_5)Mn(PH_3)_2\}_2(\mu\text{-}C_4H_2)]^+$ of the mixed-valent species $[\mathbf{7}]^+$ in various conformations (vide supra) all converged into essentially symmetric structures, i.e., with equivalent metal sites and with Mn−C and C−C bond lengths intermediate between those of the neutral and the dicationic species (Table S4 of the Supporting Information). The spin density is mainly and almost equally concentrated on the manganese centers (0.3612 and 0.3606). An appreciable amount is also found on the central carbon atoms of the C_4 backbone (0.1581 and 0.1582, respectively), while less spin density is located

Scheme 10. Conformational Analysis of 7

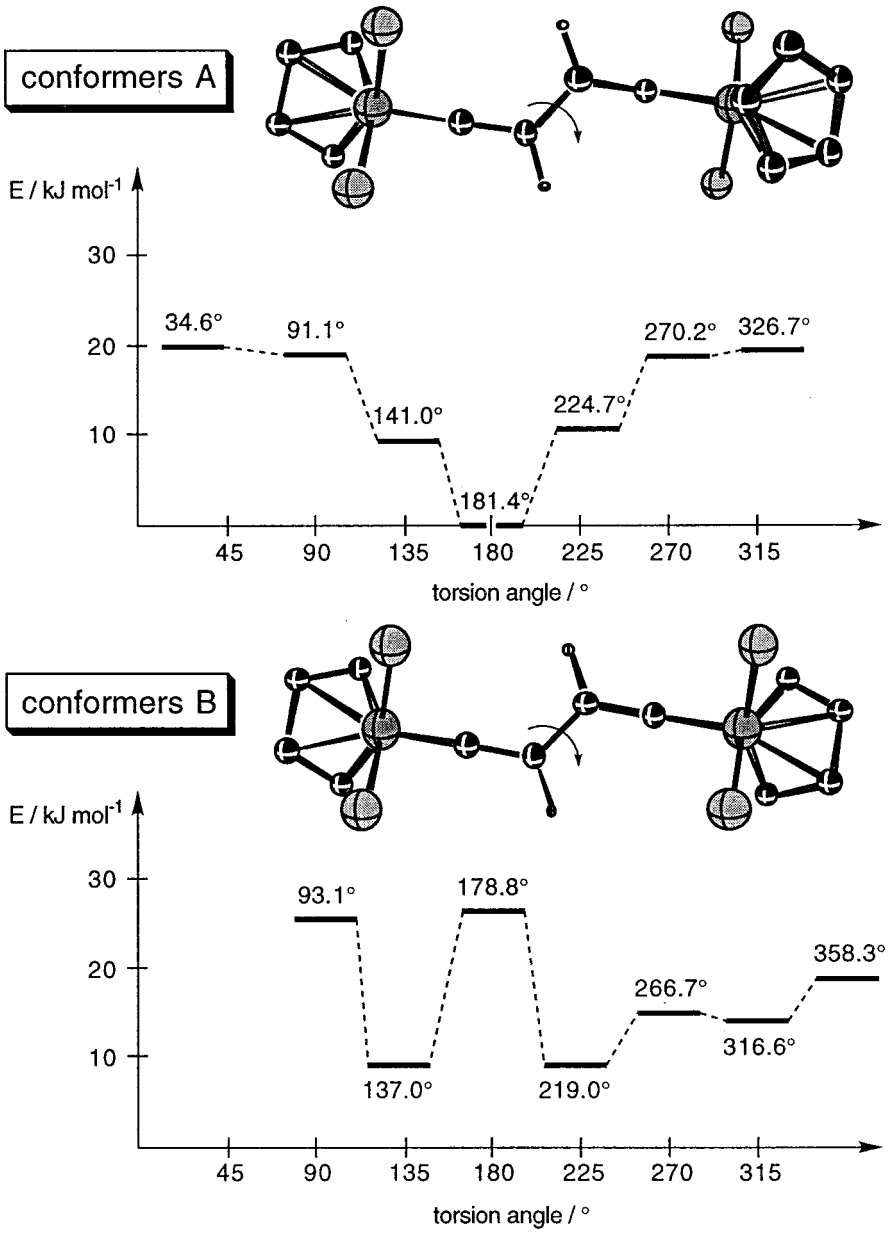

on the ligating carbon atoms (0.0280 and 0.0281, respectively). Therefore, both the geometrical parameters and the spin distribution indicate a symmetric electronic configuration, i.e., that the odd electron is delocalized between the two manganese centers in accord with the EPR measurements of $[\mathbf{7}]^+$ (vide supra).

Theoretically a quantitative estimate of the metal−metal interaction in binuclear complexes may be obtained from the difference between the first and second gas-phase ionization potentials, $\Delta IP = IP(n = 1) - IP(n = 0)$ (n = charge of the complex). The ionization potentials can be obtained via DFT calculations as the difference in total energy between the reduced species in the un-ionized initial state and the ionized final state.[49] With the calculated total energies $E(n = 0) = -243.08$ eV, $E(n = 1$, geometry of $n = 0$ complex$) = -237.95$ eV and $E(n = 2$, geometry of $n = 1$ complex$) = -229.23$ eV the ionization potentials were found to be $IP(n = 0) = E(n = 1) - E(n = 0) = 5.13$ eV and $IP(n = 1) = E(n = 2) - E(n = 1) = 8.72$ eV and accordingly $\Delta IP = 3.59$ eV. To correlate these theoretical gas-phase values with the experimentally observable oxidation potentials, especially the difference between the first and second oxidation potentials $\Delta E°$, the solvation energies of the charged complexes has to be taken into account. The solvation energies can roughly be estimated using a simple electrostatic continuum model derived by Onsager and Born.[50] The solvation energy is the sum of a dipole ($\Delta E_{solv,\mu}$) and a charge ($\Delta E_{solv,Q}$) term: $\Delta E_{solv} = \Delta E_{solv,\mu} + \Delta E_{solv,Q}$ (the full expressions are given, for example, in ref 51). The dipole moments μ were calculated via a DFT calculation; the effective cavity radius a_0 was calculated as the sum of the greatest internuclear distance plus the van der Waals

(49) Belanzoni, P.; Re, N.; Sgamellotti, A.; Floriani, C. *J. Chem. Soc., Dalton Trans.* **1998**, 1825.

(50) (a) Born, M. *Z. Phys.* **1920**, *1*, 45. (b) Onsager, L. *J. Am. Chem. Soc.* **1936**, *58*, 1486. (c) Rashin, A. A.; Honig, B. *J. Phys. Chem.* **1985**, *89*, 5588.

(51) Bickelhaupt, F. M.; Ziegler, T.; von Ragué Schleyer, P. *Organometallics* **1995**, *14*, 2288.

radii of the two atoms involved (a_0 = 15.3 Å). The expressions were evaluated using the relative dielectric constant of CH_2Cl_2 (ϵ_r = 9.08 at 20 °C), giving an approximate solvation energy contribution of ca. −3.4 eV. This leads to a $\Delta E°$ value of ∼0.2 V, which is surprisingly close to the experimental value of 0.211 V. The relatively small $\Delta E°$ is therefore the result of a large negative solvation energy of the charged species and is not indicative of electron localization.

Experimental Section

Reagent grade benzene, toluene, pentane, diethyl ether, and tetrahydrofuran were dried and distilled from sodium benzophenone ketyl prior to use. Dichloromethane was distilled first from P_4O_{10} and, prior to use, from CaH_2. Literature procedures were used to prepare the following compounds: 1,2-bis(dimethylphosphino)ethane (dmpe),[52] $(RC_5H_4)_2Mn$ (R = H, Me),[53] $(MeC_5H_4)_2Mn(dmpe)$,[10] $[(C_5Me_5)Mo(CO)_3H]$.[54] $PhC{\equiv}CSnMe_3$ and $Me_3SiC{\equiv}CSnMe_3$ were prepared by a modified literature procedure[55] (see the general procedure given below). *n*-BuLi (1.6 M in hexane) and $Me_3SiC{\equiv}CH$ were used as received; $PhC{\equiv}CH$ was freshly distilled before use. All the manipulations were carried out under a nitrogen atmosphere using Schlenk techniques or a drybox.

IR spectra were obtained on a Bio-Rad FTS-45 instrument and near-IR spectra on a Perkin-Elmer Lambda 19 UV/vis/near-IR spectrometer. NMR spectra were obtained on Varian Gemini-300 or Varian Gemini-200 spectrometers at 300 or 200 MHz for ^1H, 75.4 or 50.3 MHz for $^{13}C\{^1H\}$, 121.5 MHz for $^{31}P\{^1H\}$, and 111.9 MHz for $^{119}Sn\{^1H\}$ spectra, respectively. The ^1H NMR spectra of paramagnetic compounds were obtained from concentrated solutions of analytically pure compounds using NMR tubes (5 mm) equipped with a J. Young valve to ensure long-term exclusion of oxygen and moisture. The assignment of the ^1H NMR signals for paramagnetic compounds is principally based on the investigations of Köhler et al.[6,14] Chemical shifts for ^1H and $^{13}C\{^1H\}$ NMR spectra are given in ppm with respect to the signals of residual solvent protons (^1H) or ^{13}C atoms of the deuterated solvents. $^{31}P\{^1H\}$ NMR spectra and $^{119}Sn\{^1H\}$ NMR spectra were referenced to 85% external H_3PO_4 and external $(CH_3)_4Sn$, respectively. ($w_{1/2}$ = line width at half-height, vt = virtual triplet, $J_{PH} = {}^2J_{PH} + {}^4J_{PH}$; $J_{PC} = {}^1J_{PC} + {}^3J_{PC}$). Mass spectra were obtained with a Finnigan MAT 8430 instrument (EI and FAB) or a triple-stage Finnigan TSQ 700 quadrupole instrument (San Jose, CA), equipped with a combined Finnigan atmospheric pressure ion (API) source (ESI). Cyclic voltammogramss were obtained with a BAS 100B/W instrument (10^{-3} M in 0.1 M CH_2Cl_2/*n*-$Bu_4N(PF_6)$). X-band EPR spectra were obtained with a Varian E-6 spectrometer.

Computational Details. The calculations were carried out using the Amsterdam density functional (ADF Version 2.2.1) package developed by Baerends et al.[56] and vectorized by Ravenek.[57] The adopted numerical integration procedure was that of te Velde et al.[58] An uncontracted triple-ζ STO basis set was employed for the 3s, 3p, 3d, 4s, and 4p valence orbitals of manganese. For carbon (2s, 2p), phosphorus (3s, 3p), and hydrogen (1s) use was made of a double-ζ basis set augmented by an extra polarization function. The fully occupied inner shells of manganese and phosphorus (1s2s2p), as well as carbon (1s), were assigned to the cores and treated by the frozen-core approximation. All the geometries were calculated at the local density approximation (LDA) level[59] with the parametrization of Vosko et al.[60] The relative energies were evaluated by including Becke's nonlocal exchange[61] and Perdew's nonlocal correlation corrections.[62] All geometries were fully optimized at the quantum mechanical level without symmetry constraints. For the mixed-valence cation a broken-symmetry spin-unrestricted calculation with an unsymmetrical start-up potential was employed to avoid the problem of a constrained equal amplitude of molecular orbitals over the two metal centers and to allow the unpaired electron to localize on one center if such an arrangement is energetically favorable.

General Procedure for the Preparation of Stannylated Acetylenes $RC{\equiv}SnMe_3$ (R = Ph, $SiMe_3$). In a Schlenk tube equipped with a sintered-glass frit $RC{\equiv}CH$ (21 mmol) was dissolved in diethyl ether (20 mL). After the solution was cooled to −50 °C, a solution of *n*-BuLi in hexane (20.5 mmol) was added dropwise. The cooling bath was removed, and the mixture was allowed to reach room temperature. The resulting solution was stirred for an additional 30 min. This solution was again cooled to −30 °C, followed by addition of small portions of Me_3SnCl (20 mmol) as a solid. A white fluffy solid precipitated immediately. The resulting suspension was warmed to room temperature and stirred for an additional 1 h. The solvent was removed in vacuo until an oily suspension formed. This residue was extracted with pentane, and the extract was filtered through the glass frit. Evaporation of the solvent gave the pure stannylated acetylene $RC{\equiv}CSnMe_3$ in good yields (R = Ph, 85%; R = $SiMe_3$, 89%).

(1,2-Bis(dimethylphosphino)ethane)(η^5-methylcyclopentadienyl)(phenylethynyl)manganese(II) (1a). From $(MeC_5H_4)_2Mn$, dmpe, and $PhC{\equiv}CH$. $(MeC_5H_4)_2Mn$ (215 mg, 1.01 mmol) was dissolved in 5 mL of benzene. To the resulting red solution was added dmpe (150 mg, 1 mmol). The reaction mixture turned pale yellow. Phenylacetylene (102 mg, 1 mmol) was then added in one portion, and the mixture was stirred for 20 h. The deep red solution was evaporated to dryness. After extraction of the crude residue with pentane the solution was filtered through Celite and concentrated. Crystallization at −35 °C gave 211 mg of **1a** (54% yield) as red-brown crystals.

^1H NMR (C_6D_6): δ −20.4 ($w_{1/2}$ = 3370 Hz, PCH_3), −13.5 (PCH_2), −5.6 ($w_{1/2}$ = 587 Hz, C_5H_4), 5.6 ($w_{1/2}$ = 372 Hz, Ph *H*), 21.2 ($w_{1/2}$ = 813 Hz, Ph *H*). IR (KBr): ν 2008, 1980 cm^{-1} (C≡C). EI-MS: *m*/*z* 386 (M^+). Anal. Calcd for $C_{20}H_{28}MnP_2$: C, 62.34; H, 7.33. Found: C, 62.46; H, 7.24.

From $(MeC_5H_4)_2Mn$, dmpe, and $PhC{\equiv}CSnMe_3$. $(MeC_5H_4)_2Mn$ (108.7 mg, 0.51 mmol) was dissolved in 3 mL of benzene. To the resulting red solution was added dmpe (75 mg, 0.5 mmol). The reaction mixture turned pale yellow. $PhC{\equiv}CSnMe_3$ (132.5 mg, 0.5 mmol) was then added in one portion, and the mixture was stirred for 38 h. The deep red solution was evaporated to dryness. After extraction of the crude residue with pentane the solution was filtered through Celite and concentrated. Crystallization at −35 °C gave 41 mg of **1a** (21% yield) as red-brown crystals. The stannylated methylcyclopentadiene byproduct was identified as 1-methyl-1-(trimethylsilyl)cyclopentadiene by ^1H and ^{119}Sn NMR spectroscopy. ^1H NMR (C_6D_6): δ −0.086 (s, 9H, $Sn(CH_3)_3$, $^2J_{SnH}$ = 52.3 Hz), 2.08

(52) Burt, R. J.; Chatt, J.; Hussain, W.; Leigh, G. J. *J. Organomet. Chem.* **1979**, *182*, 203.
(53) Brauer, G. *Handbook of Preparative Inorganic Chemistry*; F. Enke: Stuttgart, Germany, 1981; Vol. III.
(54) Nolan, S. P.; Laudrun, J. T.; Hoff, C. D. *J. Organomet. Chem.* **1985**, *282*, 357.
(55) (a) Dallaire, C.; Brook, M. A. *Organometallics* **1993**, *12*, 2332. (b) Brandsmer, L. *Preparative Acetylenic Chemistry*, 2nd ed.; 1988. (c) Stille, J. K.; Simpson, J. H. *J. Am. Chem. Soc.* **1987**, *109*, 2138.
(56) Baerends, E. J.; Ellis, D. E.; Ros, P. *Chem. Phys.* **1973**, *2*, 41.
(57) Ravenek, W. In *Algorithms and Applications on Vector and Parallel Computers*; te Riele, H. J. J., Decker, T. J., van de Vorst, H. A., Eds.; Elsevier: Amsterdam, 1987.
(58) (a) Boerritger, P. M.; te Velde, G.; Baerends, E. J. *Int. J. Quantum Chem.* **1987**, *33*, 87. (b) te Velde, G.; Baerends, E. J. *J. Comput. Phys.* **1992**, *99*, 84.
(59) Gunnarson, O.; Lundquist, I. *Phys. Rev.* **1974**, *B10*, 1319.
(60) Vosko, S. H.; Wilk, L.; Nusair, M. *Can. J. Phys.* **1980**, *58*, 1200.
(61) Becke, A. D. *Phys. Rev. A* **1988**, *38*, 2398.
(62) Perdew, J. P. *Phys. Rev. Lett.* **1985**, *55*, 1655. (b) Perdew, J. P. *Phys. Rev. B* **1986**, *33*, 8822. (c) Perdew, J. P.; Wang, Y. *Phys. Rev. B* **1986**, *33*, 8800.

(s, 3H, $C_5H_4CH_3$), 5.64 (s, 2H, C*H*, J_{SnH} = 27.1 Hz), 5.77 (s, 2H, C*H*, J_{SnH} = 21.7 Hz); coupling to the different tin isotopes ^{117}Sn and ^{119}Sn is not resolved, and coupling constants are therefore given as an average. ^{119}Sn{^{1}H} NMR (C_6D_6): δ 30.3 (s, *Sn*$(CH_3)_3$).

(1,2-Bis(dimethylphosphino)ethane)(η^5-methylcyclopentadienyl)((trimethylsilyl)ethynyl)manganese(II) (2a). From ($MeC_5H_4)_2$Mn, dmpe, and $Me_3SiC{\equiv}CH$. ($MeC_5H_4)_2$Mn (234 mg, 1.1 mmol) was dissolved in 5 mL benzene. To the resulting red solution dmpe (150 mg, 1 mmol) was added. The color of the reaction mixture turned pale yellow. Trimethylsilylacetylene (100 mg, 1.02 mmol) was then added in one portion. The solution was stirred for 65 h. The orange-red colored solution was evaporated to dryness and the crude residue was extracted with pentane. Filtration through Celite, concentrating the solution and crystallization at −35 °C gave 275 mg **2a** (65% yield) as yellow-brown crystals. ^{1}H NMR (C_6D_6): δ −21.2 ($w_{1/2}$ = 1130 Hz, PC*H*$_3$), −13.4 ($w_{1/2}$ = 654 Hz, PC*H*$_2$), −5.1 ($w_{1/2}$ = 380 Hz, C_5H_4), 5.6 ($w_{1/2}$ = 165 Hz, Si(C*H*$_3)_3$). IR (KBr): ν 1945 cm^{-1} (C≡C). EI-MS: *m*/*z* 381 (M$^+$). Anal. Calcd for $C_{17}H_{32}MnP_2Si$: C, 53.53; H, 8.46. Found: C, 53.46; H, 8.11.

From ($MeC_5H_4)_2$Mn, dmpe, and $Me_3SiC{\equiv}CSnMe_3$. ($MeC_5H_4)_2$Mn (108.7 mg, 0.51 mmol) was dissolved in 3 mL of benzene. To the resulting red solution was added dmpe (72 mg, 0.48 mmol). The reaction mixture turned pale yellow. $Me_3SiC{\equiv}CSnMe_3$ (125.3 mg, 0.48 mmol) was then added in one portion. The solution was stirred for 80 h. The orange-red solution was evaporated to dryness, and the crude residue was extracted with pentane. Filtration through Celite, concentration of the solution, and crystallization at −35 °C gave 68 mg of **2a** (37% yield) as yellow-brown crystals.

(1,2-Bis(dimethylphosphino)ethane)(η^5-cyclopentadienyl)(phenyl-alkynyl)manganese(II) (1b). This complex was prepared in solution by starting from $(C_5H_5)_2$Mn, dmpe, and PhC≡CH and was identified by ^{1}H NMR spectroscopy. ^{1}H NMR (1,2-CD_2ClCD_2Cl): δ −20.6 ($w_{1/2}$ = 850 Hz, PC*H*$_3$), −13.3 (PC*H*$_2$), −5.7 ($w_{1/2}$ = 348 Hz, C_5H_5), 5.3 (Ph *H*), 21.0 (Ph *H*).

(1,2-Bis(dimethylphosphino)ethane)(η^5-cyclopentadienyl)((trimethylsilyl)ethynyl)manganese(II) (2b). This complex was prepared in solution by starting from $(C_5H_5)_2$Mn, dmpe, and $Me_3SiC{\equiv}CH$ and was identified by ^{1}H NMR spectroscopy. ^{1}H NMR (1,2-CD_2ClCD_2Cl): δ −20.9 ($w_{1/2}$ = 946 Hz, PC*H*$_3$), −13.2 ($w_{1/2}$ = 542 Hz, PC*H*$_2$), −5.2 ($w_{1/2}$ = 304 Hz, C_5H_5), 5.3 ($w_{1/2}$ = 136 Hz, Si(C*H*$_3)_3$).

[(1,2-Bis(dimethylphosphino)ethane)(η^5-methylcyclopentadienyl)(phenylethynyl)manganese(III)] Tetrafluoroborate ([1a](BF$_4$)). To a cooled solution (−50 °C) of **1a** (50 mg, 0.13 mmol) in 5 mL of dichloromethane was added a solution of [$(C_5H_5)_2$Fe](BF$_4$) (35 mg, 0.13 mmol) in 2 mL of dichloromethane. The mixture was stirred at −50 °C for 3 h. Adding diethyl ether precipitated a red-brown solid which was dissolved in dichloromethane and again precipitated with diethyl ether (2×). The precipitate was washed with cold diethyl ether (3 × 5 mL). Removal of the solvent gave 57 mg of [**1a**](BF$_4$) (93% yield) as a brownish powder. ^{1}H NMR (CD_2Cl_2, −20 °C): δ −70.5 ($w_{1/2}$ = 246 Hz, *o*-*H*), −65.8 ($w_{1/2}$ = 195 Hz, *p*-*H*), −52.4 (PC*H*$_2$), −46.3 ($w_{1/2}$ = 1095 Hz, PC*H*$_3$), −20.4 ($w_{1/2}$ = 663 Hz, C_5H_4), 42.4 ($w_{1/2}$ = 257 Hz, *m*-*H*), 49.9 ($w_{1/2}$ = 541 Hz, C*H*$_3C_5H_4$). IR (KBr): ν 2070 cm^{-1} (C≡C). FAB-MS: *m*/*z* 385 (M$^+$). Anal. Calcd for $C_{20}H_{28}BF_4MnP_2$: C, 50.88; H, 5.98. Found: C, 50.89; H, 5.65.

(1,2-Bis(dimethylphosphino)ethane)(η^5-methylcyclopentadienyl)((trimethylsilyl)ethynyl)manganese(III) Tetrafluoroborate ([2a](BF$_4$)). To a cooled solution (−50 °C) of 2a (25 mg, 0.07 mmol) in 3 mL of dichloromethane was added a solution of [$(C_5H_5)_2$Fe](BF$_4$) (18 mg, 0.07 mmol) in 1 mL of dichloromethane. The mixture was stirred at −50 °C for 3 h. Adding diethyl ether precipitated an orange solid, which was dissolved in dichloromethane and again precipitated with diethyl ether (2×). The precipitate was washed with cold diethyl ether (3 × 3 mL). Removal of the solvent gave 30 mg of [**2a**](BF$_4$) (90% yield) as a brownish powder. ^{1}H NMR (CD_2Cl_2): δ −50.1 ($w_{1/2}$ = 453 Hz, PC*H*$_2$), −42.5 ($w_{1/2}$ = 340 Hz, PC*H*$_3$), −39.1 ($w_{1/2}$ = 433 Hz, PC*H*$_2$), −28.8 ($w_{1/2}$ = 306 Hz, MeC_5H_4-2/5), −21.6 ($w_{1/2}$ = 273 Hz, PC*H*$_3$), 7.8 ($w_{1/2}$ = 95 Hz, MeC_5H_4-3/4), 11.9 ($w_{1/2}$ = 71 Hz, Si(C*H*$_3)_3$), 60.6 ($w_{1/2}$ = 406 Hz, C*H*$_3C_5H_4$). IR (KBr)): ν 1995 cm^{-1} (C≡C). ESI-MS: *m*/*z* 381 (M$^+$). Anal. Calcd for $C_{17}H_{32}BF_4MnP_2Si$: C, 43.61; H, 6.89. Found: C, 43.53; H, 6.46.

Reduction of [1a](BF$_4$). To a cooled solution (−50 °C) of [**1a**](BF$_4$) (47 mg, 0.1 mmol) in 5 mL of dichloromethane was added ($MeC_5H_4)_2$Co (21 mg, 0.1 mmol) as a solid. The mixture was stirred for 3 h at the same temperature and was then evaporated to dryness. The residue was extracted with pentane (3 × 1 mL), filtered through Celite, and concentrated. The filtrate was cooled to −80 °C to give 35 mg of **1a** (89% yield) as red-brown crystals. Spectroscopic and analytical data were identical with those obtained by the synthesis from ($MeC_5H_4)_2$Mn and phenylacetylene/dmpe as described above.

Reduction of [2a](BF$_4$). The reduction was carried out as described above using [**2a**](BF$_4$) (25 mg, 0.05 mmol) and ($MeC_5H_4)_2$Co (11 mg, 0.05 mmol) in 3 mL of dichloromethane to yield 15 mg of **2a** (80% yield) as yellow-brown crystals. Spectroscopic and analytical data were identical with those obtained by the synthesis from ($MeC_5H_4)_2$Mn and (trimethylsilyl)acetylene/dmpe as described above.

Bis(1,2-bis(dimethylphosphino)ethane)bis(phenylethynyl)manganese(II) (3). From ($C_5H_5)_2$Mn, dmpe, and PhC≡CH. A mixture of ($C_5H_5)_2$Mn (93 mg, 0.5 mmol), dmpe (150 mg, 1 mmol), and PhC≡CH (60 mg, 1.18 mmol) in 20 mL of benzene was stirred for 36 h, filtered through Celite, and evaporated to dryness. The oily deep red residue was extracted with benzene and again filtered through Celite. The filtrate was evaporated to dryness. The orange-red product **3** was washed with cold pentane and dried in vacuo to give 258 mg of **3** (93% yield). ^{1}H NMR (CD_2Cl_2): δ −14.8 ($w_{1/2}$ = 330 Hz, PC*H*$_3$), −13.6 (PC*H*$_2$), −4.0 ($w_{1/2}$ = 124 Hz, *o*-*H*), 0.4 ($w_{1/2}$ = 45 Hz, *p*-*H*), 16.6 ($w_{1/2}$ = 76 Hz, *m*-*H*). IR (KBr): ν 2008, 1975 cm^{-1} (C≡C). The spectroscopic data agree well with the literature values reported previously.[16]

From ($MeC_5H_4)_2$Mn, dmpe, and PhC≡CH. The procedure was analogous to that described above using ($MeC_5H_4)_2$Mn (107 mg, 0.5 mmol), dmpe (150 mg, 1 mmol), and PhC≡CH (60 mg, 1.18 mmol) in 5 mL of benzene. Stirring for 20 h gave 269 mg of **3** (97% yield).

From ($MeC_5H_4)_2$Mn, dmpe, and PhC≡CSnMe$_3$. Stirring a mixture of ($MeC_5H_4)_2$Mn (107 mg, 0.5 mmol), dmpe (150 mg, 1 mmol), and PhC≡CSnMe$_3$ (291 mg, 1.1 mmol) in 5 mL of benzene for 70 h followed by workup as described above gave 250 mg of **3** (90% yield).

Bis(1,2-bis(dimethylphosphino)ethane)bis((trimethylsilyl)ethynyl)manganese(II) (4). **From ($C_5H_5)_2$Mn, dmpe, and $Me_3SiC{\equiv}CH$.** A mixture of ($C_5H_5)_2$Mn (93 mg, 0.5 mmol), dmpe (150 mg, 1 mmol), and $Me_3SiC{\equiv}CH$ (116 mg, 1.18 mmol) in 20 mL of benzene was stirred for 14 h at 50 °C and then cooled to room temperature, filtered through Celite, and evaporated to dryness. The oily orange-red residue was extracted with pentane and again filtered through Celite. After the volume was reduced until the beginning of crystallization, the solution was kept at −30 °C. A 247 mg amount of **4** (90% yield) was collected as yellow crystals. ^{1}H NMR (CD_2Cl_2): δ −14.9 ($w_{1/2}$ = 256 Hz, PC*H*$_3$), −13.7 (PC*H*$_2$), 4.8 ($w_{1/2}$ = 35 Hz, Si(C*H*$_3)_3$). IR (KBr): ν 1942 cm^{-1} (C≡C). The spectroscopic data agree well with the literature values reported previously.[16]

From ($MeC_5H_4)_2$Mn, dmpe, and $Me_3SiC{\equiv}CH$. The procedure was analogous to that described above using ($MeC_5H_4)_2$Mn (107 mg, 0.5 mmol), dmpe (150 mg, 1 mmol), and $Me_3SiC{\equiv}CH$ (116 mg, 1.18 mmol) in 5 mL of benzene with stirring for 7 h at 50 °C. Recrystallization of the crude product from pentane gave 261 mg of **4** (95% yield).

From $(MeC_5H_4)_2Mn$, dmpe, and $Me_3SiC{\equiv}CSnMe_3$. Stirring a mixture of $(MeC_5H_4)_2Mn$ (107 mg, 0.5 mmol), dmpe (150 mg, 1 mmol), and $Me_3SiC{\equiv}CSnMe_3$ (287 mg, 1.1 mmol) in 5 mL of benzene for 20 h at 65 °C followed by workup as described above gave 253 mg of **4** (92% yield).

(1,2-Bis(dimethylphosphino)ethane)(η^5-methylcyclopentadienyl)(phenylvinylidene)manganese(I) (5) and (1,2-bis(dimethylphosphino)ethane)(η^5-methylcyclopentadienyl)(phenyl(tributyltin)vinylidene)manganese(I). From $(MeC_5H_4)_2Mn$, dmpe, PhC≡CH, and *n*-Bu_3SnH. $(MeC_5H_4)_2Mn$ (224 mg, 1.05 mmol) was dissolved in 5 mL of benzene. To the resulting red solution was added dmpe (150 mg, 1 mmol). The reaction mixture turned pale yellow. Phenylacetylene (102 mg, 1 mmol) was then added in one portion. After the mixture was stirred for 20 h, *n*-Bu_3SnH (291 mg, 1 mmol) was added. After for additional 60 h of stirring the volatiles were removed under reduced pressure until a red-brown oily residue was obtained. After extraction of the remaining oil with pentane and filtration through Celite, crystallization at −35 °C gave 321 mg of **5** (83% yield) as brick red crystals. The mother liquor was evaporated and dried in vacuo, yielding a red-brown oil which contained $(MeC_5H_4)Mn(dmpe){=}C{=}C(Ph)SnBu_3$ as the main product.

5. ^{1}H NMR (toluene-d_8, 10 °C): δ 0.74 (6H, vt, J_{PH} = 4.1 Hz, PCH_3), 1.11 (6H, vt, J_{PH} = 4.8 Hz, PCH_3), 1.12, 1.46 (2H × 2, m, PCH_2), 1.94 (3H, s, $C_5H_4CH_3$), 3.86, 4.30 (2H × 2, m, $C_5H_4CH_3$), 5.82 (1H, t, $^4J_{PH}$ = 8.7 Hz, =C(H)Ph), 6.83 (1H, m, Ph H), 7.16 (2H, m, Ph H), 7.25 (2H, m, Ph H). $^{31}P\{^1H\}$ NMR (toluene-d_8, 10 °C): δ 92.8 (s). $^{31}P\{^1H\}$ NMR (toluene-d_8, −98 °C): 93.1 (d, $^2J_{PP}$ = 53.8 Hz), 94.5 (d, $^2J_{PP}$ = 53.8 Hz). $^{13}C\{^1H\}$ NMR (toluene-d_8, 10 °C): δ 14.5 (s, $C_5H_4CH_3$), 21.2 (vt, J_{PC} = 6.0 Hz, PCH_3), 23.3 (vt, J_{PC} = 14.9 Hz, PCH_3), 31. (vt, J_{PC} = 21.7 Hz, PCH_2), 80.7, 84.6 (s, MeC_5H_4), 98.4 (s, *ipso*-C MeC_5H_4), 121.1, 121.7, 122.6 (s, Ph), 137.7 (s, *ipso*-C Ph), 142.2 (t, $^3J_{PC}$ = 5.2 Hz, C(H)Ph), 342.5 (t, $^2J_{PC}$ = 35.5 Hz, =C=). IR (KBr): ν 1594, 1564 cm^{-1} (C=C). EI-MS: m/z 386 (M^+). Anal. Calcd for $C_{20}H_{29}MnP_2$: C, 62.18; H, 7.57. Found: C, 61.99; H, 7.35.

$(MeC_5H_4)Mn(dmpe){=}C{=}C(Ph)SnBu_3$. ^{1}H NMR ($C_6D_6$): δ 2.14 (3H, s, $C_5H_4CH_3$), 3.97, 4.39 (2H × 2, m, C_5H_4Me). Other signals are superimposed with those of **5** and free *n*-Bu_3SnH. $^{31}P\{^1H\}$ NMR (C_6D_6): δ 93.2 (s). $^{119}Sn\{^1H\}$ NMR (C_6D_6): δ −32.4 (t, $^4J_{PSn}$ = 68.4 Hz).

From 1a and $(C_5Me_5)Mo(CO)_3H$. 1a (42 mg, 0.11 mmol) was dissolved in 3 mL of benzene. To the resulting orange-red solution was added $(C_5Me_5)Mo(CO)_3H$ (32 mg, 0.1 mmol) as a solid in small portions. The reaction mixture was stirred for 15 min. Removal of the volatiles under reduced pressure gave a deep red oily residue which was extracted with pentane. Filtration of the solution through Celite, concentration, and crystallization at −35 °C gave 34 mg of **5** (87% yield) as brick red crystals.

Oxidation of 5 to [1a](BF_4). To a cooled solution (−30 °C) of **5** (97 mg, 0.25 mmol) in 5 mL of dichloromethane was added a solution of $[(C_5H_5)_2Fe](BF_4)$ (68 mg, 0.25 mmol) in 2 mL of dichloromethane. The mixture was stirred at −30 °C for 2 h. A red-brown solid was precipitated by adding diethyl ether. The precipitate was collected and reprecipitated twice. Additionally the precipitate was washed with cold diethyl ether (3 × 5 mL). Removal of the solvent gave 100 mg of [**1a**](BF_4) (85% yield) as a brownish powder.

(1,2-Bis(dimethylphosphino)ethane)(η^5-methylcyclopentadienyl)((trimethylsilyl)vinylidene)manganese(I) (6) and (1,2-Bis(dimethylphosphino)ethane)(η^5-methylcyclopentadienyl)((trimethylsilyl)(tributyltin)vinylidene)-manganese(I). From $(MeC_5H_4)_2Mn$, dmpe, $Me_3SiC{\equiv}CH$, and *n*-Bu_3SnH. $(MeC_5H_4)_2Mn$ (234 mg, 1.1 mmol) was dissolved in 5 mL of benzene. To the resulting red solution was added dmpe (150 mg, 1 mmol). The reaction mixture turned pale yellow. (Trimethylsilyl)acetylene (100 mg, 1.02 mmol) was added in one portion. After the mixture was stirred for 65 h, tributyltin hydride (291 mg, 1 mmol) was added. The resulting solution was stirred for additional 60 h. The volatiles were removed under reduced pressure until a yellow-brown oily residue was obtained. After extraction of the remaining oil with pentane and filtration through Celite, crystallization at −80 °C gave 168 mg of **6** (43% yield) as orange-red crystals. The mother liquor was evaporated, yielding an orange-red oil which contained $(MeC_5H_4)Mn(dmpe){=}C{=}C(SiMe_3)SnBu_3$ as the main product.

6. ^{1}H NMR (C_6D_6): δ 0.31 (9H, s, Si(CH_3)$_3$), 0.85 (6H, vt, J_{PH} = 3.7 Hz, PCH_3), 1.27 (6H, vt, J_{PH} = 4.4 Hz, PCH_3), 1.30, 1.69 (2H × 2, m, PCH_2), 2.06 (3H, s, $C_5H_4CH_3$), 3.87 (2H, m, MeC_5H_4), 4.10 (1H, t, $^4J_{PH}$ = 9.1 Hz, =C(H)SiMe$_3$), 4.26 (2H, m, MeC_5H_4). $^{31}P\{^1H\}$ NMR (C_6D_6): δ 93.2. $^{31}P\{^1H\}$ NMR (toluene-d_8): δ 95.1. $^{13}C\{^1H\}$ NMR (toluene-d_8): δ 2.2 (s, Si(CH_3)$_3$), 14.2 (s, $C_5H_4CH_3$), 21.8 (vt, J_{PC} = 5.3 Hz, PCH_3), 21.8 (vt, J_{PC} = 14.5 Hz, PCH_3), 30.8 (vt, J_{PC} = 21.8 Hz, PCH_2), 79.3, 83.8 (s, MeC_5H_4), 98.3 (s, *ipso*-C MeC_5H_4), 137.5 (s, =C(H)SiMe$_3$), 339.3 (t, $^2J_{PC}$ = 32.8 Hz, =C=). IR (KBr): ν 1583, 1558 cm^{-1} (C=C). EI-MS: m/z 382 (M^+). Anal. Calcd for $C_{17}H_{33}MnP_2Si$: C, 53.39; H, 8.70. Found: C, 53.80; H, 9.04.

$(MeC_5H_4)Mn(dmpe){=}C{=}C(SiMe_3)SnBu_3$. ^{1}H NMR ($C_6D_6$): δ 2.12 (3H, s, $C_5H_4CH_3$), 3.80, 4.06 (2H × 2, m, MeC_5H_4). Other signals were superimposed with those of **6** and free *n*-Bu_3SnH. $^{31}P\{^1H\}$ NMR (C_6D_6): δ 92.8 (s). $^{119}Sn\{^1H\}$ NMR (C_6D_6): δ −23.7 (t, $^4J_{PSn}$ = 74.6 Hz).

From 2a and $(C_5Me_5)Mo(CO)_3H$. 2a (42 mg, 0.11 mmol) was dissolved in 3 mL of benzene. To the resulting orange-red solution was added $(C_5Me_5)Mo(CO)_3H$ (32 mg, 0.1 mmol) as a solid in small portions. The reaction mixture was stirred for 15 min. Removal of the volatiles under reduced pressure gave a deep red oily residue, which was extracted with pentane. Filtration of the solution through Celite, concentration, and crystallization at −80 °C gave 31 mg of **6** (80% yield) as brick red crystals.

Oxidation of 6 to [2a](BF_4). To a cooled solution (−30 °C) of **6** (69 mg, 0.18 mmol) in 5 mL of dichloromethane was added a solution of $[(C_5H_5)_2Fe](BF_4)$ (49 mg, 0.18 mmol) in 2 mL of dichloromethane. The mixture was stirred at −30 °C for 2 h. An orange solid was precipitated by adding diethyl ether. The precipitate [**2a**](BF_4) was collected and reprecipitated twice. The precipitate was washed with cold diethyl ether (3 × 3 mL). Removal of solvent gave 67 mg of [**2a**]BF_4 (79% yield) as an orange powder.

Bis[(1,2-bis(dimethylphosphino)ethane)(η^5-methylcyclopentadienyl)manganese(I)](μ-2,3-diphenylbutadien-1,4-diylidene) (7). From $(MeC_5H_4)_2Mn$, dmpe, and PhC≡CH. $(MeC_5H_4)_2Mn$ (224 mg, 1.05 mmol) was dissolved in 5 mL of benzene. To the resulting red solution was added dmpe (150 mg, 1 mmol). The reaction mixture turned pale yellow. Phenylacetylene (102 mg, 1 mmol) was added in one portion. After it was stirred for 6 weeks, the reaction mixture was filtered through Celite. Volatiles were removed from the filtrate under reduced pressure. The resulting red oily residue was extracted with pentane (3 × 5 mL) until the extracts were colorless. The red pentane extracts were collected and filtered through a Celite pad. Partial removal of the solvent under reduced pressure resulted in the initial crystallization of **7**. Additional cooling to −35 °C afforded 135 mg of **7** (35% yield) as red crystals. The mother liquor contained a mixture of **3**, **5**, and **7**. It was impossible to separate this mixture by crystallization. ^{1}H NMR (toluene-d_8, 45 °C): δ 0.83 (6H, vt, J_{PH} = 3.4 Hz, PCH_3), 1.27 (6H, vt, J_{PH} = 4.6 Hz, PCH_3), 1.15, 1.36 (2H × 2, m, PCH_2), 1.97 (3H, s, $C_5H_4CH_3$), 4.19, 4.29 (2H × 2, m, MeC_5H_4), 6.76 (1H, m, Ph), 7.12 (2H, m, Ph), 7.37 (2H, m, Ph). $^{31}P\{^1H\}$ NMR (toluene-d_8, 45 °C): δ = 95.7 (br). $^{31}P\{^1H\}$ NMR (toluene-d_8, −80 °C): δ 95.1 (d, $^2J_{PP}$ = 42.6 Hz), 97.7 (d, $^2J_{PP}$ = 42.6 Hz). $^{13}C\{^1H\}$ NMR (C_6D_6, 21 °C): δ 15.6 (s, $C_5H_4CH_3$), 22.2 (vt, J_{PC} = 5.8 Hz, PCH_3), 24.7 (vt, J_{PC} = 14.1 Hz, PCH_3), 31.3 (vt, J_{PC} = 24.0 Hz, PCH_2), 81.2, 83.9 (s, MeC_5H_4), 97.7 (s, *ipso*-C MeC_5H_4), 120.9, 123.4, 128.3 (s, Ph), 130.6 (t, $^4J_{PC}$ = 4.2 Hz, *ipso*-C Ph), 145.3 (t, $^3J_{PC}$ = 4.2 Hz,

Table 5. Crystal Data Collection and Refinement Parameters

	2a	5	7	8
formula	$C_{17}H_{32}MnP_2Si$	$C_{20}H_{29}MnP_2$	$C_{42}H_{56}Mn_2P_4 \cdot C_6H_6$	$C_{40}H_{56}B_2F_8Mn_2P_4$
color	red	red	deep red	red
cryst dimens (mm)	0.75 × 0.65 × 0.5	0.3 × 0.3 × 0.3	0.25 × 0.25 × 0.45	0.47 × 0.30 × 0.05
cryst syst	monoclinic	orthorhombic	triclinic	triclinic
space group (No.)	$P2_1/c$ (14)	*Pbca* (61)	$P\bar{1}$ (2)	$P\bar{1}$ (2)
a (Å)	14.390(2)	12.097(2)	10.225(2)	8.632(2)
b (Å)	11.180(2)	15.543(3)	13.887(2)	9.265(2)
c (Å)	15.285(2)	21.535(4)	17.246(4)	14.544(3)
α (deg)			106.37(2)	106.52(3)
β (deg)	116.30(1)		106.69(2)	100.23(3)
γ (deg)			96.53(2)	90.03(3)
V (Å^3)	2204.5(6)	4049(1)	2199.5(7)	1095.8(4)
Z	4	8	2	1
fw	381.40	386.33	848.72	944.22
d(calcd) (g cm^{-3})	1.149	1.267	1.281	1.431
abs coeff (mm$^{-1)}$	0.792	0.808	0.750	0.785
F(000)	812	1632	896	488
T (K)	203(5)	233(5)	223(5)	296(2)
2*θ* scan range (deg)	5.0 < 2*θ* < 60.0	5.0 < 2*θ* < 54.0	5.0 < 2*θ* < 50.0	3.0 < 2*θ* < 56.0
scan speed (deg min^{-1})	2.00−29.00	2.00−29.00	2.00−29.00	1.70−16.50
scan range (*ω*) (deg)	1.20	1.20	1.60	1.00 + 0.35 tan *θ*
no. of unique data	6378	4263	7661	5277
no. of data obsd ($I > 2\sigma(I)$)	3861	3085	6289	3486
abs cor	none	none	none	numerical
soln method	direct methods	Patterson	direct methods	Patterson
R1, wR2 (%)[a]	5.43, 15.5	11.3, 12.8	7.2, 13.6	5.68, 17.57
goodness of fit	1.051	1.846	1.231	1.035

[a] $R1 = \sum(F_o - F_c)/\sum F_o$ ($I > 2\sigma(I)$); $wR2 = \{\sum w(F_o^2 - F_c^2)^2/\sum w(F_o^2)^2\}^{1/2}$.

=*C*(Ph)), 342.6 (t, $^2J_{PC}$ = 35.0 Hz, =*C*=); IR (KBr): *ν* 1589 (m), 1562 (m), 1518 (s), 1498 (s) (C=C), 931 cm^{-1} (m, P−C). EI-MS: *m*/*z* 770 (M^+). Anal. Calcd for $C_{40}H_{56}Mn_2P_4$: C, 62.34; H, 7.32. Found: C, 62.46; H, 6.94.

From 8. 8 (47 mg, 0.05 mmol) was dissolved in 10 mL of dichloromethane. To the resulting pale red solution was added $(MeC_5H_4)_2Co$ (21 mg, 0.1 mmol) as a solid. The reaction mixture turned orange-red within 1 h. The reaction mixture was filtered through Celite and evaporated to dryness. The residue was extracted with pentane (3 × 3 mL) until the extracts were colorless. The red pentane extracts were collected and filtered through Celite. Slow evaporation of the solvent at room temperature resulted in crystallization of 32 mg of **7** (82% yield) as red crystals.

Bis[(1,2-bis(dimethylphosphino)ethane)(*η*^{5}-methylcyclopentadienyl)manganese(III)](*μ*-2,3-diphenylbut-2-en-1,4-diylidyne) Bis(tetrafluoroborate) (8). From 7. 7 (31 mg, 0.04 mmol) was dissolved in 3 mL of dichloromethane. To the resulting orange-red solution was added $[(C_5H_5)_2Fe](BF_4)$ (22 mg, 0.08 mmol) as a solid. The reaction mixture turned deep red within 15 min, and after 3 h it was pale red. The reaction mixture was filtered through Celite. The filtrate was concentrated by partial removal of the solvent to about half of its volume. Addition of diethyl ether caused precipitation of an orange solid. The crude product was collected, washed with diethyl ether (3 × 2 mL) to remove $(C_5H_5)_2Fe$, and dried in vacuo. Reprecipitation (2×) and crystallization from dichloromethane at room temperature by slow evaporation of the solvent gave 36 mg of **8** (95% yield) as brilliant orange crystals. ^{1}H NMR (CD_3NO_2): *δ* 1.25 (6H, vt, J_{PH} = 5.0 Hz, PC*H*$_3$), 1.54 (6H, vt, J_{PH} = 5.9 Hz, PC*H*$_3$), 1.55, 2.00 (2H × 2, m, PC*H*$_2$), 2.01 (3H, s, $C_5H_4CH_3$), 4.16, 4.26 (2H × 2, m, MeC_5H_4), 7.50−7.75 (5H, m, Ph). ^{31}P{^{1}H} NMR (CD_3NO_2): *δ* 82.6. ^{13}C{^{1}H} NMR (CD_3NO_2): *δ* 15.2 (s, $C_5H_4CH_3$), 19.9 (vt, J_{PC} = 11.9 Hz, P*C*H$_3$), 22.1 (vt, J_{PC} = 17.2 Hz, P*C*H$_3$), 31.5 (vt, J_{PC} = 21.4 Hz, P*C*H$_2$), 88.5, 94.0 (s, Me*C*$_5$H$_4$), 107.6 (s, *ipso*-C MeC_5H_4)), 131.3, 131.4, 131.6 (s, Ph), 134.7 (s, *ipso*-C Ph), 160.2 (s, =*C*(Ph)), 307.50 (t, $^2J_{PC}$ = 40.5 Hz, =*C*=). IR (KBr): *ν* 1632 (br), 1592 (w), 1576 (w), 1487 (m) (C=C), 1083 (s), 1055 (s, B−F), 931 cm^{-1} (m, P−C). ESI-MS: *m*/*z* 857 ($M^{2+}BF_4^-$), 385 (M^{2+}). Anal. Calcd for $C_{40}H_{56}B_2F_8Mn_2P_4$: C, 50.88; H, 5.98. Found: C, 51.12; H, 6.29.

From [1a](BF$_4$). [1a](BF$_4$) (142 mg, 0.3 mmol) was dissolved in 5 mL of dichloromethane. The deep red solution was stirred at room temperature for 6 weeks. Due to a high decomposition rate insoluble products were formed. After evaporation to dryness the oily black residue was extracted with dichloromethane until the extracts were colorless. These were filtered through Celite and concentrated. Crystallization from dichloromethane at room temperature by slow evaporation of the solvent gave 28 mg of **8** (20% yield) as orange crystals.

Bis[(1,2-bis(dimethylphosphino)ethane)(*η*^{5}-methylcyclopentadienyl)manganese(II^1/$_2$)](*μ*-2,3-diphenylbutadiene-1,4-diylidene) Tetrafluoroborate ([7](BF$_4$)). From 7. 7 (38.5 mg, 0.05 mmol) was dissolved in 5 mL of dichloromethane. To the resulting orange-red solution was added $[(C_5H_5)_2Fe](BF_4)$ (13.6 mg, 0.05 mmol) in 2 mL of dichloromethane. The reaction mixture turned green-red within 30 min. The solvent was removed in vacuo, and the residue was washed with diethyl ether to remove $(C_5H_5)_2Fe$. The crude product was dissolved in 5 mL of dichloromethane, and the solution was filtered through Celite. Addition of diethyl ether caused precipitation of a green solid, which was again dissolved in dichloromethane and precipitated with diethyl ether, giving 30 mg (70% yield) of [**7**](BF$_4$).

From 8. 8 (47.2 mg, 0.05 mmol) was dissolved in 5 mL of dichloromethane. To the resulting light red solution was added $(MeC_5H_4)_2Co$ (11.0 mg, 0.05 mmol) in 2 mL of dichloromethane. The reaction mixture turned green-red within 30 min. The solvent was removed in vacuo, and the crude product was dissolved in dichloromethane, filtered through Celite, and crystallized at −30 °C, giving 17 mg (40% yield) of [**7**](BF$_4$). EPR (CH_2Cl_2; −190 °C): g = 2.018, $A(^{55}Mn)$ = 60 G. Near-IR (CH_2Cl_2): *λ* 1018 nm ($\epsilon = 3.3 \times 10^3$ M^{-1} cm^{-1}).

X-ray Structural Analyses of 2a, 5, 7, and 8. The data were collected on a Siemens P4 (**2a**), Siemens P3 (**5**, **7**), and

(63) (a) Sheldrick, G. M. SHELXS-86; University of Göttingen, Göttingen, Germany, 1986. (b) Sheldrick, G. M. SHELXL-93; University of Göttingen, Göttingen, Germany, 1993.

Enraf-Nonius CAD-4 (**8**) diffractometers. Solution and refinement were performed using the SHELXS-86 and SHELXL-93 software packages, respectively.[63] Crystal data collection and refinement parameters are given in Table 5. The rather poor *R* values for the structure determination of **5** are due to the lack of an absorption correction and the irregular shape of the crystal.

Acknowledgment. We thank the Swiss National Science Foundation for support of this work.

Supporting Information Available: Tables S1−S4, giving the DFT calculations, and additional material concerning the X-ray structure analyses of the complexes **2a**, **5**, **7**, and **8**, including complete listings of X-ray parameters, bond lengths and angles, and positional and thermal parameters. This material is available free of charge via the Internet at http://pubs.acs.org.

OM9810549